Department of Diagnostic Radiology
Helsinki University Central Hospital
University of Helsinki, Finland

MAGNETIC RESONANCE IMAGING OF FOCAL LIVER LESIONS

Characterization with the Spin Lock Technique and Detectability with Tissue-Specific Contrast Agents

Juha Halavaara

Academic Dissertation

To be presented with the permission of
the Faculty of Medicine of the University of Helsinki,
for public discussion in **Auditorium XIII**.

On November 8th, 2002, at 12 noon.

Helsinki 2002

Supervisor

Docent Sören Bondestam
Department of Diagnostic Radiology
University of Helsinki

Reviewers

Docent Pekka Niemi
Department of Diagnostic Radiology
University of Turku

Professor Sanjay Saini
Department of Radiology
Massachusetts General Hospital and Harvard Medical School
Boston, USA

Opponent

Docent Osmo Tervonen
Department of Diagnostic Radiology
University of Oulu

ISBN 952-91-5218-3 (print)
ISBN 952-10-0761-3 (pdf)
Yliopistopaino
Helsinki 2002

“You’ll Never Walk Alone…”

To Sari and the Boys

CONTENTS

LIST OF ORIGINAL PUBLICATIONS

My thesis is based on the following articles and in the text, they are referred to as their Roman numerals I-V.

I. Halavaara JT, Sepponen RE, Lamminen AE, Vehmas T, Bondestam S. Spin lock and magnetization transfer MR imaging of focal liver tumors. Magn Reson Imaging 1998; 16:359-364.

II. Halavaara JT, Lamminen AE, Bondestam S, Sepponen RE, Tanttu JI. Differentiation of hepatic hemangiomas and metastases with multiple slice spin lock MR imaging. Br J Radiol 1995; 81:395-403.

III. Halavaara JT, Lamminen AE, Bondestam S, Standertskjöld-Nordenstam C-G, Hamberg LE. Detection of focal liver lesions with superparamagnetic iron oxide: value of STIR and SE imaging. J Comput Assist Tomogr 1994; 18:897-904.

IV. Halavaara JT, Lamminen AE. MnDPDP as a negative contrast agent: evaluation of STIR imaging compared to T1-weighted SE and GE techniques. J Comput Assist Tomogr 1997; 21:94-99.

V. Halavaara J, Tervahartiala P, Isoniemi H, Höckerstedt K. Efficacy of sequential use of superparamagnetic iron oxide and gadolinium in liver MR imaging. Acta Radiol 2002; 43:180-185.

Permission for reprinting was requested from the Publishers.

SYMBOLS AND ABBREVIATIONS

m	magnetic moment
r	spin density
B_0	main magnetic field
B_1	RF field
B_{1L}	locking field
CNR	contrast-to-noise ratio
CSF	cerebrospinal fluid
CT	x-ray computer assisted tomography
CTAP	CT during arterial portography
E_{MT}	magnetization transfer effect
E_{SL}	spin lock effect
f_0	frequency
FA	flip angle
FISP	fast imaging with steady state free precession
FLAIR	fluid attenuated inversion recovery
FNB	fine needle biopsy
FNH	focal nodular hyperplasia
FOV	field of view
fSE	fast spin echo
Gd-BOPTA	gadolinium benzyloxypropionictetraacetic acid
Gd-DOTA	gadolinium tetraazacyclododecanetetraacetic acid
Gd-DTPA	gadolinium diethylenetriamine pentaacetic acid
Gd-EOB-DTPA	gadolinium-ethoxybenzyldiethylenetriaminepentaacetic acid
GE	gradient echo
HASTE	half-fourier acquisition single shot turbo spin echo
HCC	hepatocellular carcinoma
IR	inversion recovery
MA	matrix
Mn	manganese
MnDPDP	manganese dipyridoxyl-diphosphate
MRA	magnetic resonance angiography

MRI	magnetic resonance imaging
MRS	magnetic resonance spectroscopy
MT	magnetization transfer
MTC	magnetization transfer contrast
NEX	number of excitations
NMR	nuclear magnetic resonance
RES	reticuloendothelial system
RF	radiofrequency
ROI	region-of-interest
SAR	specific absorption rate
SD	standard deviation
SEM	standard error of the mean
SE	spin echo
SI	signal intensity
SIR	signal intensity ratio
SL	spin lock
SNR	signal-to-noise ratio
SPIO	superparamagnetic iron oxide
STIR	short inversion time inversion recovery
T1	longitudinal relaxation time
T1ρ	relaxation time in the rotating frame of reference
T2	transverse relaxation time
TA	time of acquisition
TE	time to echo
TI	inversion time
TL	locking time
TR	repetition time
USPIO	ultrasmall superparamagnetic iron oxide

INTRODUCTION

Liver is a common site for distant metastases of cancers originating from the colon and the breast. Liver cirrhosis is often complicated by hepatocellular carcinoma. Modern operative techniques and local therapies such as radiofrequency (RF) ablation are effective methods to treat liver metastases or primary hepatic malignancies (Fong et al., 1997; Gazelle et al., 2000). Therefore, the determination of liver lesion count, and the nature of the lesion are important. At present, the most accurate noninvasive method for the assessment of liver lesion count is magnetic resonance imaging (MRI).

The contrast between tissues on MR images depends mainly on differencies in their T1 and T2 relaxation times and proton densities. Basic techniques such as spin echo (SE) or gradient echo (GE) sequences can be used for imaging to obtain high contrast images. Additionally, there are a number of other methods to manipulate MR contrast in order to enhance signal differencies between normal and pathological tissues.

The magnetization transfer (MT) technique in MRI was introduced in 1989 (Wolff and Balaban, 1989). The method is based on saturating macromolecular spins with a dedicated irradiation radiofrequency (RF)-pulse, and observing the effects of the subsequent exchange processes. The signal of tissues with a high macromolecular content is reduced on MT images in comparison to the standard images. MT based tissue contrast may even more effectively be generated with the spin lock (SL) technique which probes tissue relaxation processes at very low magnetic field strengths while maintaining the high signal-to-noise ratio provided by the polarizing magnetic system (Sepponen et al., 1984). In a SL experiment, a preparation or locking pulse is applied before the signal collecting conventional imaging sequence. The multiple slice SL imaging technique was introduced in 1993 (Sepponen et al., 1993).

Contrast agents are widely used in routine clinical MR imaging. Extracellular gadolinium chelates such as gadolinium diethylenetriamine pentaacetic acid (Gd-DTPA) or gadolinium tetraazacyclododecanetetraacetic acid (Gd-DOTA) constitute the major group of MR contrast agents used today. Because of their unspecific nature with rapid extracellular distribution, fast imaging techniques and knowledge about the different enhancement patterns of liver lesions are essential. More recently, research has focused on the development of tissue-specific MR contrast agents with

a long imaging window due to their prolonged removal from the target-tissue. The accumulation of magnetically potent agents in normal hepatic parenchyma while leaving liver tumors unaffected increases the signal difference between tumors and normal liver, thus rendering lesions more conspicuous. Superparamagnetic iron oxide (SPIO) and manganese (II) N,N´-dipyridoxylethylenediamine-N,N´-diacetate-5,5´-biphosphate or manganese dipyridoxyl-diphosphate (MnDPDP) are examples of tissue-specific agents.

In this thesis, a resistive 0.1T magnet and superconducting MR systems operating at 1.0T and 1.5T were used for evaluating patients with known or suspected focal liver lesions. The ability of the multiple slice SL technique in the generation of MT-like tissue contrast, and the potential of the multiple slice SL technique in the differentiation of hepatic hemangiomas and liver metastases were assessed (I, II). The benefit of tissue-specific contrast agents SPIO (III) and MnDPDP (IV) and SPIO in conjunction with Gd-DOTA in lesion detection (V) was also investigated.

REVIEW OF THE LITERATURE

1. Image Contrast in MRI

1.1 Basic principles

There are two kinds of spin relaxations. The recovery of longitudinal magnetization is characterized by the relaxation time constant T1. The dissappearance of rotating (transverse) magnetization is characterized by the relaxation time constant T2. The contrast seen on MR images is generated mainly through differencies in these tissue T1 and T2 relaxation times and to a lesser degree, through tissue spin density (Wehrli et al., 1984). In addition to these intrinsic determinants of tissue contrast, there are a number of extrinsic factors that may be employed to modify image contrast. These include the strength of the main magnetic field (Rinck et al., 1988), sequence parameters such as repetition time (TR), echo time (TE) and flip angle (FA), the use of special imaging techniques such as MT or SL, and the use of MR contrast agents (Villafana, 1988).

1.1.1 Spin echo sequence

With spin echo (SE) technique, an initial excitation pulse at resonance is applied to tilt the spins around the axis of the excitatory magnetic field (B_1). Longitudinal magnetization is reduced and transverse magnetization is generated but it starts to disappear rapidly because of spin dephasing. After a time period one half of TE, a refocusing pulse is applied and after another one half of TE an echo is produced. TE is the time from the excitatory pulse to center of the signal collection, and TR is the time between two excitations (between two excitatory pulses).

The combination of selected TR and TE determines whether images have so-called T1- or T2-weighting (Villafana 1988; Makow, 1989). T1-weighted SE images are acquired with a combination of short TR and short TE. Liver has a T1 relaxation time of approximately 550-700 ms at 1.5T (Thomsen et al., 1990; van Lom et al., 1991), 450 ms at 1.0T (Bottomley et al., 1984), and 200 ms at 0.1T (Kajander et al., 1996). By using the SE technique, T1-weighted images are obtained with a TR less than the liver T1 relaxation time. On T1-weighted images, fluid such as the content of a simple liver cyst has low signal intensity because of long T1 relaxation time, whereas fat appears bright due to short T1 relaxation time.

On T2-weighted MR images obtained with proper imaging parameters, tissues with long T2 relaxation times such as simple liver cysts or hemangiomas appear bright. T2-weighted SE images are obtained with a long TE and with a long TR (Villafana, 1988; Makow, 1989). Liver T2 relaxation time is approximately 45-60 ms (Goldberg et al., 1991). Therefore, with a TE of 90 ms or more, liver signal has decayed significantly. TR on the other hand should be long enough to allow recovery of tissue magnetization (at least three times tissue T1 relaxation time).

1.1.2 Gradient echo sequence

With gradient echo (GE) techniques, gradient inversions are employed in order to rephase the spins (Villafana, 1988). Generally, short TRs and TEs are employed. Also, small flip angles are utilized to take advantage of residual longitudinal magnetization to acquire images with high signal intensity despite of very short TRs. Flip angle affects image contrast in conjunction with TE. With a given TR, the use of a large FA and short TE, sequences produce predominantly T1-weighted images, and with the use of small FAs and a long TE, the images have predominantly T2-weighting (Wehrli, 1987).

1.1.3 Inversion recovery sequence

With inversion recovery (IR) sequences, the magnetization of protons is initially flipped 180°. Then, the magnetization begins to recover, but after a time called inversion time (TI), a 90° RF pulse is applied, and regular signal collecting sequence follows. Because of tissue T1 dispersion i.e. tissue T1 relaxation time dependence on the main magnetic field (B_0) strength (Koenig et al., 1984), the TI and TR used with the IR sequences should be correctly chosen according to B_0 for the best contrast (Young et al., 1998). By adjusting the TI approximately to 0.7 times of tissue T1 relaxation time, it is possible to almost completely cancel signal from selected tissues (Bydder and Young, 1985). One widely used clinical IR application is the fluid attenuated inversion recovery (FLAIR) sequence for nulling the signal from cerebro-spinal fluid (CSF) for enhanced detection of brain white matter abnormalities (de Coene et al., 1992).

The short inversion time IR sequence (STIR) is a sequence with TI so short that the signal from fat is nulled (Bydder et al., 1985a and 1985b). With a long TE, the STIR technique possesses synergistic T1 and T2 contrast properties, and gives high signal for most pathological lesions such as liver metastases or hemangiomas that exhibit both long T1 and long T2 (Atlas et al., 1988). In clinical MRI, the STIR sequence has proved to be sensitive in the detection of focal liver lesions (Paling et al., 1988; Reinig et al., 1989). At 1.5T, it has been shown to be as sensitive as CT during arterial portography (CTAP) (Paulson et al., 1994).

2. Methods to Improve Image Contrast: Radiofrequency Pulse Manipulation

2.1 General considerations

There are a number of extrinsic methods to improve contrast in MR images. Important clinical applications include the MT and the SL techniques. MT has been utilized in liver tumor imaging (Outwater et al., 1992; Kahn et al., 1993) as well as in the imaging of knee (Wolff et al., 1991), head and neck tumors (Markkola et al., 1996), spine (Finelli et al., 1994) and brain (Lundbom, 1992). It is also utilized in MR angiography (MRA) (Atkinson et al., 1994). The SL technique has been used in the MR imaging of muscle (Lamminen et al., 1993) and breast diseases (Santyr et al., 1989), in head and neck MR imaging (Markkola et al., 1996), in neuroradiology (Aronen et al., 1999), and in MR histology (Engelhardt and Johnson, 1996).

2.2 Magnetization transfer technique

The MT technique was first introduced as a method for producing additional contrast for MR imaging by Wolff and Balaban in 1989 (Wolff and Balaban, 1989). In tissues, there are freely moving protons in water molecules (H_f) and protons with restricted mobility (H_r) located in macromolecules. There is constant exchange of magnetizations between these proton pools due to dipole-dipole interactions (Koenig et al., 1978; Grad and Bryant, 1990). Tissue contrast in MT imaging technique is based on these exchange processes. MT utilizes often an off-resonance RF pulse for saturation of the magnetization of bound protons before the signal generating and collecting MR sequence. Due to exchange processes, the saturation of H_f is transferred to H_r. Therefore, there is a net reduction in the magnetization of H_f, and consecutively, a decrease in the strength of the collected signal. With tissues with high macromolecule content such as liver the

detected reduction in signal intensity is high while in tissues such as fat, the MT effect is minimal. The observed decline in signal intensity is therefore tissue-dependent (Niemi et al., 1992), which is the basis of the magnetization transfer contrast (MTC).

2.3 Multiple slice spin lock technique

The efficiency of relaxation mechanisms is known to increase when the main magnetic field decreases due to water-macromolecule interactions (Koenig et al., 1984). SL MR imaging technique utilizes the measurement of longitudinal relaxation at very low magnetic field strengths (far below 0.01T). In an on-resonance SL experiment, the spins are first excited by a 90° RF pulse. Thereafter, a locking pulse (B_{1L}) at resonance is implemented. The magnetization remains locked in the direction of B_{1L} for the locking time (TL) period and thus, the relaxation occurs along the direction of B_{1L} (Sepponen, 1992). This relaxation is characterized by the time constant T1ρ. The value of T1ρ depends on the strength of the locking field B_{1L} (T1ρ dispersion) (Sepponen et al., 1986; Lamminen et al., 1993; Markkola et al., 1996). Typically, T1ρ is approximately T1 at very low magnetic field strengths, and close to T2 at field strengths of B_0. It has been suggested that MT is the major source of relaxation at very low magnetic field strengths (Zhong et al., 1989; Grad et al., 1990; Zhong et al., 1990; Koenig et al., 1993; Henkelman et al., 1993), and it has been demonstrated that T1ρ is sensitive to MT effects between mobile water protons and macromolecular protons in proteins.

The multiple slice SL technique was introduced by Sepponen and co-workers in 1993 (Sepponen et al., 1993). This technique has been demonstrated to produce high contrast images with T1ρ weighting (Santyr et al., 1994). Locking pulses consisting of three sections are applied. First section tilts the magnetization 90° from the direction of the main magnetic field. Then, the locking period is followed and the magnetization is locked by B_{1L} and the relaxation takes place. The magnetization is returned back to the direction of the main magnetic field by applying the third section. After the introduction of the locking pulse, the signal is collected by applying a conventional imaging sequence (Sepponen, 1992). Thus, high signal-to-noise is maintained with the use of the multiple slice SL method.

It has been suggested that in tissues with a high protein content such as liver, MT is the dominant relaxation mechanism detected with the SL technique (Zhong et al., 1989). MT imaging has been shown to be useful in the distinction between hepatic hemangiomas and liver metastases (Kahn et al., 1992; Outwater et al., 1992; Loesberg et al., 1993). Therefore, it can be expected that the SL technique may be used to obtain images with improved liver/lesion information when compared with conventional sequences. As the SL technique generates more efficiently MT based tissue contrast, and with the possibility of T1ρ dispersion through changing the locking field, the SL technique has theoretical advantages over the MT technique.

3. Methods to Improve Image Contrast: MR Contrast Agents

The purpose of contrast agents in liver MRI is to increase the signal difference between normal hepatic parenchyma and focal liver lesion, thus lowering the threshold for detection. Accurate delineation of pathological processes and improved lesion characterization potential are additional but equally important aims of contrast agent use.

3.1 Basic principles of MR contrast agents

A number of MR contrast agents have been developed. Basically, they can be divided into extracellular (unspecific) and cell-targeted (tissue-specific) agents depending on their biodistribution within the body. According to their physiologic behavior, they may be classified as extracellular, hepatobiliary, reticuloendothelial system (RES), blood pool and hybrid agents. The latter includes gadobenate dimeglumine (Gd-BOPTA) and gadolinium-ethoxybenzyldiethylenetriaminepentaacetic acid (Gd-EOB-DTPA) which can be imaged in the extracellular and hepatocyte phases. Contrast agents alter tissue T1 and T2 relaxation rates to the extent that a measurable change in signal intensity is observed. Paramagnetic and superparamagnetic ions or compounds have such properties.

Paramagnetic substances possess unpaired electrons, which have magnetic moments. When placed in an external magnetic field, these unpaired electrons align parallel to the field, thus reinforcing the external field. The mechanisms of paramagnetic contrast agents on proton relaxation have widely been studied. The magnitude of the magnetic interaction between a paramagnetic compound and neighboring water protons is proportional to the inverse of the distance raised to the sixth power

($1/r^6$). Thus, it is essential that water protons have access to the vicinity paramagnetic ions. In addition, the relaxation effect is proportional to the square of the magnetic moment.

Superparamagnetism can occur if a crystal containing regions of unpaired spins are large enough (Bean and Livingstone, 1959). Such particles possess a net magnetic moment, which is by magnitude larger than the sum of its individual unpaired electrons. When placed in an external magnetic field the magnetic moments of these particles align parallel with the field. The magnetic moments of these particles are much greater than the magnetic moments of paramagnetic agents. Due to the inhomogeneities within the magnetic field caused by these particles, the nearby diffusing spins demonstrate rapid dephasing resulting in decreased signal intensity in clinical images.

3.2 Gadolinium derivatives

Gadolinium chelates were the first contrast agents available for clinical abdominal MR imaging (Carr et al., 1984). Paramagnetic gadolinium increases tissue relaxation rates. Tissues where it accumulates are seen brighter in the enhanced T1-weighted images than in the unenhanced images. Gadolinium chelates are extracellular contrast agents with pharmacokinetical characteristics similar to iodine contrast agents used with x-ray computer assisted tomography (CT) (Mahfouz and Hamm, 1997). After intravenous injection, it rapidly accumulates both into the interstitium of normal liver and solid hepatic lesions. At a given time point their signal intensity may be equal. Therefore, fast imaging techniques with accurate timing are necessary when using extracellular contrast agents. Dynamic gadolinium-enhanced MRI has shown potential in the characterization of liver lesions (Mitchell et al., 1994) while the benefit in lesion detection is negligible (Hamm et al., 1992).

3.3 Tissue-specific contrast agents

In developing tissue-specific contrast agents for liver tumor imaging, the goal has been to produce agents that accumulate in normal tissue but not in focal lesions. The signal from normal liver changes while they have practically no effect on the signal acquired from e.g. metastatic liver deposits. The aim is that the signal difference, i.e. the contrast-to-noise ratios (CNR) of these lesions increase. Therefore, tissue-specific agents have the potential to decrease the detection threshold. Another advantage of liver-specific contrast agents is a long imaging window. Imaging may take place even several hours after the contrast agent injection. Also, the doses needed are much smaller

than with Gd-DTPA. In clinical MRI, three different tissue-specific contrast agents are currently available namely SPIO, MnDPDP and Gd-BOPTA.

3.3.1 Superparamagnetic iron oxide

Superparamagnetic iron oxide (SPIO) (Endorem®, Guerbet, Paris, France) was the first tissue-specific contrast agent introduced for liver MRI (Saini et al., 1987; Stark et al., 1988; Tsang et al., 1988; Fretz et al., 1989; Weissleder et al., 1989). It is selectively targeted to the RES, and it accumulates in the Kupffer cells within the liver (Saini et al., 1987; Weissleder et al., 1989). The Kupffer cells constitute about 80% of the RES. Thus, of a given dose of SPIO a large part eventually ends up within liver parenchyma. SPIO is a superparamagnetic contrast agent. SPIO particles are large enough to act as independent magnetic domains (Stark, 1990). They create magnetic fields around themselves when placed within an external magnetic field. Therefore, they promote small field inhomogeneities within the external magnetic field and hence, tissue T2-relaxivity increases due to the rapid dephasing of the spins (Gillis and Koenig, 1987). Through this so-called susceptibility effect, the signal from normal liver dramatically decreases after SPIO administration. While malignant liver foci do not contain Kupffer cells, their signal remains unaltered, and the signal difference between liver and lesions increases. The effective imaging window after a slow SPIO-infusion is from approximately 30 minutes to several hours (van Hecke et al., 1989).

SPIO consists of iron oxide particles that are 120-180 nm in diameter. The particles are suspended in water, and then coated with dextran in order to form a stable compound. It is administered as a slow intravenous infusion. SPIO is biodegradable and the iron is eventually incorporated into normal iron metabolism of the body (Weissleder et al., 1989). Maximum increase in 1/T2 (i.e. T2 relaxation rate) occurs approximately four hours after administration, and the half-time of the 1/T2 effect is 1-2 days (Weissleder et al., 1989). The half-life of the iron is approximately 3 days. Liver signal normalizes after SPIO infusion within 3-7 days (Saini et al., 1987; Stark et al., 1988).

SPIO-enhanced MRI has shown potential in lesion detection (Reimer et al., 2000). Several reports have demostrated increased lesion counts in SPIO-enhanced images at 1.0T or less (Fretz et al., 1990; Seneterre et al., 1996; Ward et al., 2000) and in 1.5T (Winter et al., 1993; Bellin et al., 1994; Oudkerk et al., 1997; Müller et al., 1999; Poeckler-Schoeniger et al., 1999). However, contradictory

reports are available (Marchal et al., 1989; Denys et al., 1994; Duda et al., 1994). There is also evidence that the use of SPIO may improve lesion characterization. Focal nodular hyperplasia (FNH) may reliably be diagnosed with the use of SPIO (Precetti-Morel et al., 1999; Paley et al., 2000). Double-contrast imaging with SPIO in conjunction with Gd-DTPA has also been suggested with favourable results (Nakamura et al., 2000; Ward et al., 2000; Kubaska et al., 2001).

3.3.2 Manganese dipyridoxyl-diphosphate

Manganese dipyridoxyl-diphosphate (MnDPDP) is an additional hepatobiliary contrast agent designed for liver tumor imaging (Young et al., 1990; Elizondo et al., 1991; Lim et al., 1991; Bernardino et al., 1992; Hamm et al., 1992). There is evidence of uptake of the compound to a small degree also by pancreas (Gehl et al., 1991), adrenal glands (Mitchell et al., 1995) and kidneys (Rofsky and Earls, 1996). Manganese (Mn) is a transition metal containing five unpaired electrons as Mn^{2+} ion. In order to reduce the high toxicity of manganese it is complexed to the dipyridoxyl-diphosphate (DPDP) ligand. This ligand is a B6-vitamin derivative facilitating the uptake of the compound by the hepatocytes via a membrane transport system (Rofsky and Earls, 1996). MnDPDP (Teslascan®, Nycomed, Oslo, Norway) is a stable, highly water soluble chelate. The manganese is eliminated from the body mainly through biliary excretion into the gut and via urinary excretion (Elizondo et al., 1991).

MnDPDP is a paramagnetic agent, thus enhancing the T1 relaxation of normal liver parenchyma. The observed signal intensity of normal liver increases in T1-weighted images. Metastatic liver lesions do not contain hepatocytes, and their signal intensity remains unchanged. Therefore, the signal difference between normal liver parenchyma and metastases increases (Hamm et al., 1992). The effective imaging window after MnDPDP injection is from 15 minutes to several hours (Nelson et al., 1991).

Numerous clinical studies have demonstrated the effectiveness of MnDPDP-enhanced liver MRI in lesion detection (Bernardino et al., 1991; Rummeny et al., 1991; Hamm et al., 1992). MnDPDP has also potential in lesion characterization. It has been demonstrated that MnDPDP accumulates into liver pathologies of hepatocellular origin such as FNH (Coffin et al., 1999) and well-differentiated hepatocellular carcinoma (HCC) (Ni et al., 1993).

3.3.3 Gadobenate dimeglumine

Gadolinium benzyloxypropionictetraacetic acid (Gd-BOPTA or gadobenate dimeglumine, MultiHance®, Bracco, Rome, Italy) is another currently available paramagnetic MR contrast agent with tissue-specificity. It has only 2-5% uptake into hepatocytes but more powerful effect on the T1-relaxivity than Gd-DTPA. It may also be considered as an extracellular hepatobiliary contrast agent (de Haen and Gozzini, 1993). Therefore, it is a dual acting (i.e. hybrid) contrast agent with features of extracellular compounds for dynamic imaging and accumulation into hepatocytes for delayed imaging (Kirchin et al., 1998).

3.4 MR contrast agents under development

There are numerous different intravenous MR contrast agents under investigation. Gadolinium-ethoxybenzyldiethylenetriaminepentaacetic acid (Gd-EOB-DTPA) is an ionic and water soluble gadolinium-chelate. It accumulates in the hepatocytes with approximately 50% uptake of the injected dose. As a paramagnetic substance it is used with T1-weighted sequences. Liver signal in T1-weighted images is not attenuated as much as without Gd-EOB-DTPA resulting in increased signal intensity in images. Gd-EOB-DTPA demonstrates a biphasic pattern of hepatic enhancement. At first, hepatic enhancement is unspecific reflecting liver perfusion. It is followed by the parenchymal phase of enhancement as the contrast agent is taken up by the hepatocytes (Reimer et al., 1996).

In addition to hepatobiliary agents, targeted contrast media offer an alternative approach for MRI. Gupta and Weissleder have written a thorough review of these agents (Gupta and Weissleder, 1996). The target may be a pathological process such as inflammation or hepatic metastasis. Receptor targeted compounds have been investigated (Reimer et al., 1990). Carrier molecules include antibodies such as monoclonal antibodies (Gupta and Weissleder, 1996), and proteins such as asialoglycoprotein (Reimer et al., 1991). Additionally, red blood cells have been used to transport magnetic labels to their destination (Johnson et al., 1998). The magnetic labels carried by the molecules or cells are responsible for the magnetic effects detected by MRI. These labels are metal ion chelates such as gadolinium, manganese, iron or dysprosium, and iron oxides such as magnetite or maghemite. More recently, new gadolinium-based contrast agents have been under development.

Such agents include macrocyclic gadolinium chelates (Marinelli et al., 2000) and gadoversetamide (Rubin et al., 1999).

Blood pool contrast agents have also been under investigation (Adzamli et al., 1997; Johnson et al., 1998). Ultrasmall superparamagnetic iron oxide (USPIO) are analogous to SPIO. The smaller particle size of USPIO when compared to SPIO (means sizes of 11.4 nm and 150 nm, respectively) facilitates much longer plasma half-life (approximately 81 minutes for USPIO and 6 minutes for SPIO) because phagocytosis is significantly slower due to the smaller size (Saini et al., 2000). Blood pool agents may be utilized in lesion characterization providing information about the vascular pattern of the tumor. There is no blood pool agent currently available for clinical use.

4. MRI of Liver Tumors

4.1 General considerations

The first clinical liver MRI studies were carried out by Doyle et al. and Smith et al. in 1981. In their case report with a 0.04T MR device, Smith et al. demonstrated a liver tumor having the same T1 relaxation time with blood and consequently, this tumor was diagnosed to be a hemangioma (Smith et al., 1981a). This was verified in operation. Later in 1981, Smith et al. published a liver NMR study with a population of 50 patients, and concluded that the specificity of MRI based on T1 relaxation time calculations is superior to that of ultrasound and radionuclide studies (Smith et al., 1981b). In their work, Doyle et al. (Doyle et al., 1981) studied both focal liver lesions and diffuse liver diseases. They found the specificity of T1 calculations to be lower than that suggested by Smith et al. However, they predicted that NMR may make a valuable contribution to the diagnosis of liver disease.

Abdominal MRI has for a long time been deterred by movement artifacts from heart, pulsation of the abdominal vessels, peristalsis and breathing. The introduction of high field MR devices with breathhold imaging sequences, and the introduction of dedicated phased-array body coils have made abdominal MRI attractive (Hayes et al., 1992; Campeau et al., 1995). Additionally, dynamic gadolinium-enhanced imaging during breathhold, and the possibility to acquire thin slices have substantially increased the sensitivity of liver MRI. Moreover, the number of imaging techniques with variable imaging parameters to be selected make liver MRI a challenging method. With the

invention of tissue-specific contrast agents, and special imaging techniques such as MT (Wolff and Balaban, 1989) and SL (Sepponen, 1984), effective abdominal MRI may be performed even at low magnetic field strengths far below 1.0T.

Focal liver lesions are frequently detected in patients undergoing abdominal investigations. These liver tumors constitute a major diagnostic challenge for radiological imaging especially when cancer patients are involved. Some liver lesions such as FNH occasionally appear isointense with liver parenchyma with conventional MR pulse sequences (Mortelé et al., 2000). Therefore, contrast manipulation or the use of contrast agents is often mandatory for the accurate determination of lesion count.

In the differentiation between benign and malignant liver tumors various quantitative methods have been proposed. Differencies in the T1 or T2 relaxation times (Smith et al., 1981a and 1981b; Ohtomo et al., 1985; Goldberg et al., 1991; McFarland et al., 1994) or in the signal intensity ratios (SIR) (Itoh et al., 1990) were thought to accurately make the distinction between hemangiomas and metastases. The enhancement pattern with Gd-DTPA is highly specific for hepatic hemangiomas (Mitchell et al., 1994). Rim-enhancement with peripheral wash-out sign is indicative for a malignant lesion (Mahfouz et al., 1994; Mitchell et al., 1994). A number of qualitative features including the sharpness of lesion border (Ros et al., 1987), the signal intensity characteristics (Yamashita et al., 1994), and the strength of signal with strongly T2-weighted sequences (Brown et al., 1991) have also been assigned in the characterization of liver tumors.

4.2 Imaging techniques

Optimal imaging protocol for liver tumor MR imaging depends on the field strength of the MR unit used. At low and mid-field magnetic strengths such as 0.1T or 0.5T, T1-weighted sequences are more sensitive in lesion detection than T2-weighted techniques (Reinig et al., 1989). Bottomley et al. (Bottomley et al., 1986) have demostrated that the T1 differencies between normal liver and tumor are reduced as the magnetic field strength increases. At higher field strengths, T2-imaging is more favorable (Stark et al., 1986; Foley et al., 1987). With the development of fatsuppression techniques, T2-weighted sequences with fatsuppression has been found effective liver MRI (Lu et al., 1994; Powers et al., 1994).

For good quality MR imaging of the liver, the coils are important. Earlier, whole-volume body coils were used but later, dedicated phased-array multicoil systems have been introduced (Hayes et al., 1992). With the use of these new coils, the signal-to-noise, the lesion-to-liver contrast and thus, lesion detection is considerably improved (Campeau et al., 1995). Additionally, strong and fast gradient coils enable thin slices to be acquired during breathhold.

It is obvious that a combination of sequences is required for adequate liver evaluation. In high field strengths, we need T2-weighted sequences for accurate lesion detection, and T1-weighted techniques for the depiction of anatomy, and for Gd-DTPA. Furthermore, both T1- and T2-weighted sequences are essential for the utilization of tissue-specific contrast agents. Finally, there are MR techniques such as MT and SL designed for contrast manipulation.

4.3 Focal liver lesions

Focal liver lesions range from benign cysts to extremely aggressive hepatocellular carcinomas and cholangiocarcinomas. Liver is a common site of distant metastases from a variety of cancers. The natural courses of these liver tumors are highly variable. Liver biopsy is often the ultimate conclusive diagnostic procedure but non-invasive imaging may determine lesion count and the nature of lesion(s) with high confidence level. MRI has shown its diagnostic power with respect to these demands.

4.3.1 Benign liver tumors

4.3.1.1 Liver cyst

Liver cysts are most often found as incidental findings. As a rule, cysts are easily differentiated from either other benign or malignant liver lesions. They appear as homogeneous and sharply demarcated, non-enhancing lesions with hypointensity on T1-weighted images and strong hyperintensity on T2-weighted images.

4.3.1.2 Hepatic hemangioma

The often clinically silent hepatic hemangioma is the most common solid benign liver tumor with the occurrence of up to 20% in autopsy material in Finland (Karhunen, 1986). It may be found at any age and predominantly in women. Hemangioma is usually a solitary lesion with a peripheral subcapsular location. Cavernous hemangiomas are comprised of blood-filled spaces or vascular channels lined with a single layer of endothelium separated by fibrous septa. There may be areas of thrombosis or fibrosis. Occasionally calcifications are present. Very slow blood flow is characteristic. In general, hemangiomas are stable lesions except during pregnancy when they may enlarge (Kinnard et al., 1995). Unless for the large size causing symptoms such as abdominal pain or risk of spontaneous rupture, operative treatment is not warranted.

On MR images, hemangiomas appear as sharply demarcated focal lesions with homogeneous signal intensity. With T1-weighted sequences they appear as lesions with lower signal relative to normal liver parenchyma. On T2-weighted images, however, hemangiomas demonstrate a markedly bright signal (Brown et al., 1991). The signal intensity is characteristically of the same magnitude as that of the CSF (Wittenberg et al., 1988). The highly specific feature of hemangiomas is their contrast enhancement pattern (Mitchell et al., 1994). At early contrast uptake phase, hemangiomas show peripheral nodular enhancement with typical progressive fill-in with time. Complete contrast enhancement occurs later except for giant hemangiomas with fibrous central scar tissue. Recently, atypical early homogenous enhancement (Marti-Bonmati et al., 1999) or even inside-out pattern (Kim et al., 2000) have been reported.

4.3.1.3 Focal nodular hyperplasia

Focal nodular hyperplasia (FNH) is a benign tumorlike condition that is likely a hyperplastic response to an underlying arteriovenous malformation. If cysts are excluded, it is the second most common benign hepatic tumor with the occurrence of 8% in autopsy material (Karhunen, 1986). FNH is more common in women than in men. FNH consists of nodules of hyperplastic hepatocytes containing bile ductules with abundance of vessels especially in the central scar. Due to good vascularity, necrosis is rarely seen. In MR images, FNH usually appears as a well-circumscribed solitary lesion without a capsule and with homogeneous signal-intensity. The signal-intensity in both T1 and T2-weighted images may be close to that of the normal liver parenchyma (Mattison et

al., 1987). Strong early enhancement after intravenous administration of Gd-DTPA is essential in the MR diagnosis of FNH (Mahfouz et al., 1993). The enhancement decreases with time, and FNH often appears isointense with normal liver parenchyma in late gadolinium-enhanced images. FNH demonstrates uptake of SPIO and MnDPDP due to the Kupffer cells and normally functioning hepatocytes (Vogl et al., 1993; Poeckler-Schoeniger et al., 1999). Because of the lack of complications, FNH rarely requires surgery.

4.3.1.4 Hepatic adenoma

The majority of rare hepatocellular adenomas are detected in women of childbearing age, and they are associated with the use of oral contraceptives (Karhunen, 1986). Hepatic adenomas are considered to be premalignant tumors and therefore, the treatment of choice is surgery although the risk of conversion to malignancy is considered to be small (Gordon et al., 1986). Surgery is also warranted because of the possible hemorrhagic complications (Leese et al., 1988). Adenomas consist of neoplastic hepatocytes arranged in sheets or cords, and they often present a capsule containing large vessels. Areas of hemorrhage or infarction may be detected. Fatty degeneration of the hepatocytes is frequently seen. Adenomas lack portal and terminal hepatic veins. With MRI, their signal intensity is heterogenous on both T1- and T2-weighted images (Paulson et al., 1994). On T1-weighted images, areas of increased signal intensity relative to normal live parenchyma are due to fatty degeneration or hemorrhage (Arrive et al., 1994; Chung et al., 1995). Early arterial enhancement with extracellular contrast agents may be seen (Chung et al., 1995). MR imaging findings of hepatic adenomas are, however, variable and unspecific (Rummeny et al., 1989), and thus it is often difficult to distinguish adenoma from well-differentiated hepatocellular carcinoma.

4.3.1.5 Other benign liver tumors

Other more infrequent benign liver tumors include biliary hamartomas, inflammatory pseudotumor of the liver, lipomas, angiomyolipomas, leiomyomas, and regenerative nodules in cirrhotic livers and hemangioendotheliomas in children. Focal fatty degeneration may also appear as a tumorous mass (Kawashima et al., 1986).

4.3.2 Malignant liver tumors

4.3.2.1 Liver metastases

Liver metastases are by far the most common malignant liver tumors (Baker et al., 1995). Colon, breast, lungs, stomach, and pancreas are among the primary cancers frequently followed by liver metastases. The majority of liver metastases are hypovascular i.e. they are less vascular than normal liver parenchyma. These lesions are best detected during the portal venous phase of enhancement as the liver exhibits the strongest parenchymal enhancement. Hypervascular metastases, however, may be obscured during this phase (Low et al., 1993). These lesions are more vascular than normal liver, and they demonstrate early arterial enhancement when liver is still practically unenhanced. Hypervascular metastases arise from cancers originating from kidney, breast, islet cell, skin (melanoma), adrenal gland (pheochromocytoma), and thyroid gland. Liver metastases from carcinoid and sarcomas are also hypervascular.

Hepatic metastases have a wide variety of appearances on MR images. On T2-weighted MR images metastases usually appear hyperintense relative to liver. However, their signal intensities are typically lower when compared to cysts or hemangiomas (Lewis and Chezmar, 1997). They have often heterogeneous signal intensity. On unenhanced T1-weighted images they are hypointense except for occasional melanoma metastases which may appear bright (Lee et al., 1992), and demonstrate low signal on T2-weighted images due to melanin (Lewis and Chezmar, 1997). Metastases demonstrate unsharp demarcation relative to surrounding liver parenchyma, and on T2-weighted images, they may exhibit smooth central area of high signal intensity surrounded by a ring of lower signal intensity (so called target pattern) (Laing and Gibson, 1998). Central necrosis with high T2 signal intensity is commonly seen especially in expanding and large metastases. Metastases may also appear as a mass surrounded by a ring or wedge of high signal intensity (so called halo pattern) (Lee et al., 1991). This halo pattern has been attributed to peritumoral edema or peritumoral tumor infiltration.

Metastases show heterogeneous enhancement. Rim-enhancement with peripheral washout sign in dynamic gadolinium-enhanced imaging has been reported to be highly suggestive to a malignant lesion such as metastasis (Mahfouz et al., 1994; Mitchell et al., 1994). The washout sign is seen as peripheral hypointensity relative to tumor center on delayed contrast enhanced images. Tissue-

specific contrast agents render liver metastases readily detectable because they do not enhance with these agents as normal liver parenchyma (Hamm et al., 1992; Bellin et al., 1994). A case report, however, demonstrated uptake of MnDPDP by liver metastases from neuroendocrine pancreatic tumor (Mathieu et al., 1999).

4.3.2.2 Hepatocellular carcinoma

Hepatocellular carcinoma (HCC) often occurs in association with chronic liver disease such as cirrhosis or hepatitis (Ohtomo 1997). It is the most common primary liver malignancy. The average age at diagnosis is from 60 to 80 years. The evolution of HCC is thought to happen through regenerative nodules converting to adenomatous hyperplasia which in turn may contain atypical cells or even malignant cells (Arakawa et al., 1986). Regenerative nodules are a reparative response to cell injury in cirrhosis and adenomatous hyperplasia are markedly enlarged regenerative nodules (Arakawa et al., 1986). HCC may be solitary or multiple. Large masses often present daughter lesions and necrosis is frequently seen. HCC may invade portal veins, hepatic veins or bile ducts (Nakashima et al., 1983).

The signal characteristics of HCC lesions is highly variable in both T1- and T2-weighted images (Kelekis et al., 1998). High signal on unenhanced T1-weighted image is due to intratumoral steatosis, copper accumulations (Ebara et al., 1986; Ebara et al., 1991) or hemorrhage (Kadoya et al., 1992). High signal intensity on T2-weighted images is the rule, and a mosaic pattern is often seen especially if the lesion is more than 3cm in diameter (Kadoya et al., 1992). High T2 signal intensity may be used to differentiate HCC from regenerating nodules which classically have low T2 signal attributed to iron accumulations (Buetow and Midkiff, 1997). HCC may demonstrate strong enhancement with gadolinium at early arterial phase. At later phases heterogenous contrast enhancement appearance is most often seen which is due to hypervascularity and areas of necrosis (Buetow and Midkiff, 1997). It has been demonstrated that well-differentiated HCC enhances with MnDPDP suggesting that the fagocytic activity of the hepatocytes in this type of tumor is preserved (Liou et al., 1993).

4.3.2.3 Other primary liver malignancies

Intrahepatic cholangiocarcinoma arises from the bile duct epithelium, and it is the second most common primary liver malignancy. Central scar tissue may be seen but hemorrhage, necrosis, and cystic degeneration are uncommon (Ros, 1994). Typical MR appearance is a nonencapsulated tumor with hypointensity on T1-weighted images and hyperintensity on T2-weighted images. On T2-weighted images, a hypointense central scar may be seen. With dynamic gadolinium-enhanced imaging, small tumors may show homogeneous enhancement but in large cholangiocarcinomas minimal or moderate peripheral enhancement is detected with progressive and concentric filling in (Vilgrain et al., 1997; Worwattanakul et al., 1998).

Fibrolamellar carcinoma is a rare variant of HCC with quite unique features (Berman et al., 1988). It is seen in non-cirrhotic livers of young population. Hemorrhage or necrosis are not typical. Macroscopically it resembles FNH. On MR images they are usually seen as hypointense lesions with T1-weighted sequences and hyperintense lesions with T2-weighted techniques. They have a central scar which is of low signal intensity with both T1-weighted and T2-weighted images in contrast to the cenral scar seen in FNHs which is bright on T2-weighted images (Ichikawa et al., 1999). On dynamic gadolinium-enhanced images, fibrolamellar carcinoma demonstrates early diffuse heterogeneous enhancement and promptly thereafter the enhancement is homogeneous, and isointense signal intensity is noted (McLarney et al., 1999). One reported case with MnDPDP-enhancement has been published (Ichikawa et al., 1999).

Biliary cystadenocarcinoma, hepatic angiosarcoma, epitheloid hemangioendothelioma, lymphoma and nonvascular sarcomas such as leiomyosarcoma, malignant fibrous histiocytoma and fibrosarcoma represent additional but very rare primary liver malignancies.

PURPOSES OF THE STUDY

In this thesis, focal liver lesions were investigated with the application of intrinsic and extrinsic methods for the manipulation of MR tissue contrast.

The intrinsic contrast modifying techniques were studied at 0.1T. The potential of the multiple slice spin lock (SL) technique in the distinction between hepatic hemangiomas and liver metastases was evaluated. The specific aims were:

1. To evaluate the ability of the multiple slice SL technique in the generation of magnetization transfer (MT)-like tissue contrast in liver and in focal liver lesions (I).

2. To assess the tissue characterization potential of the multiple slice SL technique (II).

The extrinsic methods were studied at the field strengths of 1.0T and 1.5T. The potential of liver-specific contrast agents in the detection of focal hepatic lesions was investigated. The specific aims were:

3. To investigate the sensitivity of liver-specific MR contrast agents superparamagnetic iron oxide (SPIO) and manganese dipyridoxyl-diphosphate (MnDPDP) in liver tumor detection. Especially, the performance of the short inversion time inversion recovery sequence (STIR) in conjunction with SPIO and MnDPDP was assessed (III, IV).

4. To evaluate the lesion detection potential of the combined use of liver-specific SPIO and extracellular gadolinium tetraazacyclododecanetetraacetic acid (Gd-DOTA) in liver MRI (V).

MATERIALS AND METHODS

1. Patient Population

A total of 92 patients were examined in this investigation.

In the Study I, twenty-seven patients with previously detected focal liver lesions were imaged. Fourteen patients with hepatic hemangiomas, and thirteen patients suffering from liver metastases of breast cancer (n=9) or colon carcinoma (n=4) were included. There were 22 women and 5 men, their ages ranging from 31 to 82 years (mean, 53 years). The lesion size in the hemangioma group ranged from 10 to 50 mm (mean, 24.4 mm), and in the metastasis group from 10 to 48 mm (mean, 20.6 mm). Three of the hemangiomas were verified with fine needle biopsies (FNB), histological proof was obtained from one hemangioma, one was observed during laparotomy, and the remaining nine cases showed typical US and/or contrast-enhanced CT appearances with no progression during follow up (from 10 to 58 months, mean 16.4 months). Two of the metastatic lesions were verified with FNBs, and histological proof was obtained from another two lesions. The remaining nine metastatic lesions were detected in patients with a known primary cancer, and these lesions showed progression during follow up.

In the Study II, sixteen patients with a known primary malignancy in the breast (n=11) or the colon (n=5) and with metastatic lesions in the liver, previously detected with ultrasound (US) or computed tomography (CT), were imaged. One of these patients had a coincidental hemangioma, which was included in the analysis. In addition, sixteen patients with hemangioma of the liver were investigated. There were thirteen women and four men in the hemangioma group, their ages ranging from 33 to 74 years (mean 53.8 years); and 13 women and three men in the metastasis group with ages ranging from 32 to 82 years (mean 57 years). The lesion size ranged from 10 to 61 mm in the hemangioma group (mean 23.5 mm) and from 10 to 48 mm in the metastasis group (mean 21.9 mm). Three hemangiomas were verified with FNBs, and one was determined during laparotomy. The remaining thirteen lesions had typical US appearances and showed no progression during follow-up (study interval range from 4 to 36 months; mean 10.5 months). Three metastases from breast cancer were verified with FNBs; eight had a typical target lesion appearance in US. The previous radiological studies (US and/or CT) in these patients had been considered normal with respect to the liver, and these lesions showed progression during follow-up. Three of the metastases

from colon carcinoma were verified with histological samples; the other two lesions were considered as new lesions and showed progression during follow-up.

In the Study III a total of 20 patients were included. One patient did not demostrate liver lesions at MRI. Eleven of the analyzed patients were males and eight were females (one patient did not demonstrate lesions in MRI). Their ages ranged from 27 to 77 years (mean, 57 years). Fifteen patients had metastatic disease from primary cancer of the colon (n=10), the kidney (n=3), the lung (n=1) or the retroperitoneum (n=1). There were one hepatocellular carcinoma and one hepatic hemangiosarcoma. Two patients had benign lesions: one with a hemangioma, the other demonstrated both a hemangioma and a focal nodular hyperplasia (FNH). The natures of the lesions were confirmed by biopsies with 12 patients. Clinical proof (increased carcinoembryonic antigen level, history of previously operated and confirmed metastases, and/or the appearance of new focal liver lesions not detected in previous examinations) was obtained from eight patients. In all metastatic cases, the type of primary malignancy had been determined from histological samples.

In the Study IV, the patient population included 15 women and 5 men their ages ranging from 49 to 76 years (mean, 62 years). Fifteen patients had metastatic liver disease (nine with primary colorectal carcinoma, three with primary breast carcinoma, and single cases with primary broncho-alveolar carcinoma, cystadenocarcinoma and cholangiocarcinoma). There were five patients with a hepatic hemangioma. The analyzed lesions ranged in diameter from 15 to 61 mm (mean, 30 mm). Ten of the metastatic cases were histologically or cytologically verified and five lesions appeared to be new lesions and showed progression during follow-up. Three hemangiomas were verified with fine needle biopsies and two had typical US appearances and showed peripheral filling-up enhancement chracteristics in dynamic contrast-enhanced CT.

In the Study V, fourteen women and six men with ages ranging from 26 to 78 years (mean, 54 years) were included. Sixteen of them demonstrated focal liver lesions: there were three patients with FNHs, two with hemangiomas and HCCs, one patient with a cholangiocarcinoma, and nine with liver metastases. There was one patient with both liver metastases and hemangiomas. With the metastatic cases, the primary cancers were in the colon (n=6) and in the breast (n=1). Additionally, there were two patients with melanoma. The lesions were verified with histology (n=12) and with imaging findings and follow-up data (n=5).

2. MR Imaging

Clinical MR devices operating with three different magnetic field strengths were used in the studies. The multiple slice SL and MT experiments (I, II) were performed by using a solenoidal coil and a resistive whole body scanner operating at 0.1T (Merit, Picker Nordstar, Helsinki, Finland). The studies with tissue-specific MR contrast agents (III-V) were conducted by using superconducting MR systems at 1.0T (III, IV) (Magnetom 42SP; Siemens, Erlangen, Germany) and at 1.5T (V) (Magnetom Vision, Siemens, Erlangen, Germany).

Moderately T2-weighted GE technique was employed in the multiple slice SL experiments (I-II). Both conventional GE and SL-GE sequences with 1500/40 ms (TR/TE, respectively) were obtained. A FA of 60° was used, and the slice thickness was 10 mm. There were two acquisitions (number of excitations, NEX=2), a 461 mm field of view (FOV), matrix (MA) size of 256x256 pixels, and time of acquisition (TA) of 12’48’’. The strength of B_{1L} was 40μT and TL was 10 ms.

In the MT experiments (I) conventional MT-GE sequence with following parameters was used: TR=1500, TE =40 ms, FA=60°, 10 mm slice thickness, NEX=2, a 461 mm FOV, MA=256x256 pixels. The amplitude of the saturation pulse B_{off} was 13μT. A 4kHz frequency offset was selected in order to avoid direct (bleedover) effect of the off-resonance pulse on the magnetization of H_f. Pulse duration of 300 ms was chosen to achieve significant MT-effect in liver parenchyma.

In the SPIO study (III), four MR pulse sequences were used. T1-weighted SE sequence was used with following parameters: TR=550 ms, TE=15 ms, NEX=6, slice thickness 8 mm with an interslice gap of 30%, FOV=350 mm, MA=192x256 pixels. T2- and proton density-weighted double echo SE sequence parameters were: TR/TEs=1900/15,90 ms, NEX=2, slice thickness 8 mm with an interslice gap of 30%, FOV=350 mm, and with MA=128x256 pixels. The STIR sequence was obtained with TR/TE/TI of 1900/20/150 ms, respectively and NEX=2, slice thickness 10 mm with an interslice gap of 50%, FOV=320 mm, MA=128x256 pixels. Saturation pulses were used cranial (all sequences) and caudal (all except the T1-weighted sequence) to the liver.

In the MnDPDP study (IV), the T1-weighted SE images were obtained with TR=600 ms and TE=17 ms, NEX=4, and MA=128x256 pixels. The T1-weighted breath-hold GE (fast low-angle shot,

FLASH) images were acquired with TR=153 ms, TE=6 ms, FA=70°, NEX=1, and MA=192x256 pixels. The STIR images were obtained with 1900/20/150 ms (TR/TE/TI), NEX=2, and MA=128x256 pixels. The precontrast T2-weighted SE images were acquired with TR=1900 ms, TE=90 ms, NEX=2, and MA 128x256 pixels. The FOV was from 350 mm to 400 mm, and the slice thickness was 10 mm with all sequences.

In the study V, TR=6.3 ms and TE=3.0 ms were used with the True FISP sequence. Additional parameters were: FA=70°, NEX=1, slice thickness=5 mm, FOV=263x350 mm, MA=192x256 pixels and TA=13 s. The T2-weighted HASTE sequence with fatsuppression consisted of TR=4.2 ms and TE=59 ms with FA=140°, NEX=1, slice thickness=6 mm, FOV=270x432 mm, MA=128x256 pixels and TA=25 s. The fatsuppressed T1-weighted sequence was used with following parameters: TR=85.2 ms, TE=4.1 ms, FA=70°, NEX=2, slice thickness=5 mm, FOV=263x350 mm, MA=140x256 pixels and TA=24 s. The fast SE-STIR sequence was used with a TI=180 ms. Additional parameters included TR=3250 ms, TE=85 ms, FA=180°, NEX=3, slice thickness=8 mm, FOV 323x430 mm, MA=150x256 pixels and TA=4 min 57 s.

3. Contrast Agents

Superparamagnetic iron oxide (SPIO, Endorem®, Guerbet, Paris, France) was used in Studies III and V. It was administered at a dose of 15 µmol/kg. In the Study III, the dose used for each patient was 0.075 ml of particle solution/kilogram body weight (mean 5.2 ml, range 3.9 to 9.0 ml), and it was diluted with 100 ml of saline. The contrast medium was infused slowly at the rate of approximately 3-4 ml per minute into the cubital vein. The postcontrast MRI was performed from 43 to 161 minutes (mean, 103 minutes) after the cessation of the SPIO infusion. Also in study V, a slow cubital vein infusion was performed. The postcontrast SPIO-enhanced MRI was conducted not earlier than 30 minutes after the the infusion. The doses (15 µmol/kg which is 0.075 ml of particle solution/kilogram body weight) ranged from 4.2 to 7.7 ml (mean, 5.5 ml). When used in conjuntion with Gd-DOTA, the SPIO-infusion was performed first followed by the bolus injection of Gd-DOTA.

In the study IV, MnDPDP was introduced as an intravenous infusion at a dose of 5 µmol/kg body weight over a time period of 20 minutes (infusion rates between 1.3 and 4.3 ml/min, mean 2.0 ml/min). Postcontrast MRI was performed 30-60 minutes after the end of the infusion.

Gadolinium tetraazacyclododecanetetraacetic acid (Gd-DOTA, Dotarem®, Guerbet, Paris, France) was used in the study V with a bolus injection into the cubital vein. A dose of 1.5 ml per kg body weight was administered. Then, a set of dynamic image series were acquired at 20, 40 and 60 seconds postinjection.

4. Image Analysis

Only one lesion of each patient was included in the quantitative analysis, except the patients with two kinds of lesions (described above). In studies I-IV, signal intensities (SI) from the lesions were obtained by using the standard region-of-interest (ROI) technique. Representative ROIs were acquied from liver parenchyma, hepatic lesions and from the background noise. In studies I-III, only lesions ≥ 10 mm were included in the analysis in order to minimize partial volume averaging effects since the section thickness of most of the sequences was 10 mm. In study IV, only lesions ≥ 15 mm were included in the quantitative analysis. ROIs covering all except the periphery of the lesion were selected. Noise was measured in the phase-encoding direction ventral to the patient. The equations used in the calculations are provided in the Appendix.

In the SPIO study (III), three radiologists independently evaluated the MR images. Total lesion count and the counts of lesions over and below 1 cm in diameter were assessed. In the MnDPDP study (IV), two radiologists evaluated the MR images. The images were evaluated by counting the lesions on a sequence-by-sequence basis, with separate sessions for each sequence in a randomized order to minimize bias for any sequence. Whether a consensus was not reached, the lesion was excluded from the final lesion count. In the study V, the efficacies of imaging techniques with and without MR contrast agents were assessed by determining the lesion counts for each technique by consensus reading of the MR images.

5. Statistical Analysis

In study I, the Friedman nonparametric two-way analysis of variance (ANOVA) was used and the subsequent post hoc analyses were performed with the use of Student-Newman-Keuls test. Statistical analysis between the SL and MT effects was conducted by using the nonparametric Wilcoxon signed rank test, and a p-value < 0.05 was considered to indicate statistical significance. In the multiple slice SL experiment (II) paired Student's t-test was used, and a p-value < 0.01 was considered to indicate statistical significance.

In study III, the paired Student's t-test was used. A p-value < 0.01 was considered to indicate statistical significance. In study IV, statistical analysis was performed by using randomized blocks analysis of variance to compare the mean CNR values for the sequences and contrast states, using the patient as a randomized block. Least squares means were compared only if the overall test of the seven mean CNR values for sequences combined with contrast states was significant, by using t-tests. A t-test was also applied for the lesion count analysis. A p-value < 0.05 was considered to indicate statistical significance. In the study V, ANOVA was used and then, the subsequent post hoc analyses were performed with the use of Student's t-test. A p-value < 0.05 was considered to indicate statistical significance.

RESULTS

1. Multiple Slice Spin Lock Technique (I-II)

The SL-effects for the liver parenchyma and the liver lesions are calculated as shown in the Appendix. Therefore, the lower the value the greater the SL-effect and vice versa. Additionally, the term SL-effect indicates the magnitude of signal loss in tissue caused by the application of the locking pulse.

The results are calculated from 32 livers with 16 hemangiomas and 16 metastases. The SL-effects of liver parenchyma (mean±SD=0.43±0.03, range 0.37-0.51) and liver metastases (mean±SD=0.43±0.06, range 0.34-0.57) were similar. The calculated SL-effects were significantly smaller in hemangiomas (mean±SD=0.53±0.03, range 0.46-0.61) ($p < 0.0001$).

The differentiation between hepatic hemangiomas and liver metastases could be established with an 91% diagnostic accuracy by using a cut-off value 0.5 for lesion SL-effect.

2. Magnetization Transfer Technique (I)

The MT-effects are calculated as shown in the Appendix. Therefore, the lower the value the greater the MT-effect and vice versa. Additionally, the term MT-effect indicates the magnitude of signal loss in tissue caused by the application of the saturation pulse.

The results are calculated from 32 livers with 16 hemangiomas and 16 metastases. The MT-effects of the liver parenchyma were 0.54±0.07 (mean±SD; range 0.39-0.66) which were nearly the same as the MT-effects of the liver metastases (mean±SD=0.57±0.10, range 0.39-0.83). The MT-effects of the hemangiomas were greater (mean±SD=0.71±0.07, range 0.59-0.85). The difference between the MT-effects of hemangiomas and normal liver parenchyma was statistically significant ($p<0.02$) while the MT-effects between liver parenchyma and metastases did not demonstrate statistical significance ($p>0.5$).

With a cut-off value for lesion MT-effect=0.7, the calculated diagnostic accuracy for the MT technique was 85% in the differentiation between hemangiomas and metastases. The SL and MT-effects of the hemangiomas and metastases with the cut-off lines are presented in **Figures 1 and 2**.

Figure 1. A plot demonstrating the SL-effects of the hepatic hemangiomas and liver metastases with the cut-off line (SL-value of 0.5). Note the small overlap between the hemangiomas and metastases.

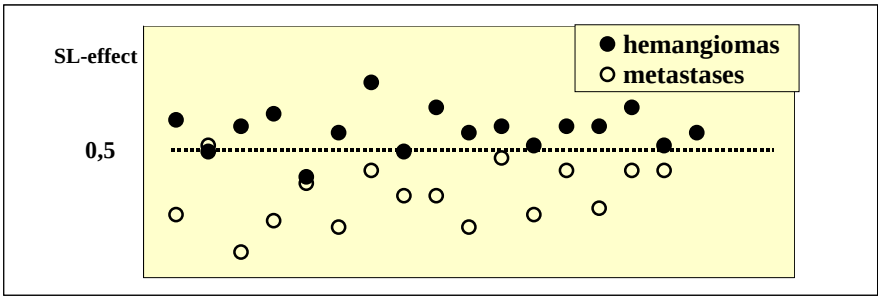

Figure 2. A plot demonstrating the MT-effects of the hemangiomas and liver metastases with the cut-off line (MT-value of 0.7). Note the slightly greater overlap of the lesions when compared to the respective SL-effects in **Fig 1**.

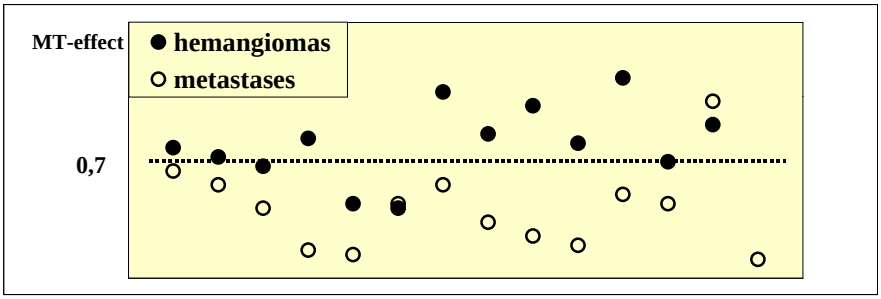

3. Superparamagnetic Iron Oxide (III)

SPIO demonstrated a powerful effect on the signal intensity of normal liver parenchyma with the use of all MR sequences. The decrease in signal intensity was greatest by using conventional T2-weighted sequence (80%). Negative hepatic enhancement (signal loss in the liver parenchyma) with the STIR sequence was 70%. The proton-density and T1-weighted SE sequences demonstrated smaller effects of 60% and 40%, respectively. The liver signal-to-noise ratios (SNR) decreased with all MR techniques (**Table 1**). The signal from liver tumors remained practically unchanged. The measured CNR ratios with the use of the different sequences with and without SPIO-enhancement are presented in **Table 2**. The increases in CNR when unenhanced and SPIO-enhanced techniques are compared to one another are also included.

The numbers of detected focal liver lesions increased significantly ($p<0.05$) by using SPIO. SPIO-enhanced MRI revealed 31% more lesions when compared to the precontrast MRI (106 and 81 lesions, respectively). Especially, 28% more lesions under 1 cm in diameter were detected with the postcontrast MRI than with the nonenhanced MRI (59 and 46 lesions, respectively). This difference demonstrated statistical significance ($p<0.05$).

Examples of SPIO-enhanced MR images are provided in **Figures 3 and 4**.

Figures 3a and b. (**a**) Unenhanced STIR image demonstrating a large mass lesion in the left liver lobe, and some vague hyperintensity in the right liver lobe. (**b**) SPIO-enhanced STIR image obtained from the same section level as in Fig. 3a. The large mass lesion is more clearly demarcated, and the small right liver lobe lesion is now easily detectable. At operation, both lesions proved to be metastases from kidney carcinoma.

3a.

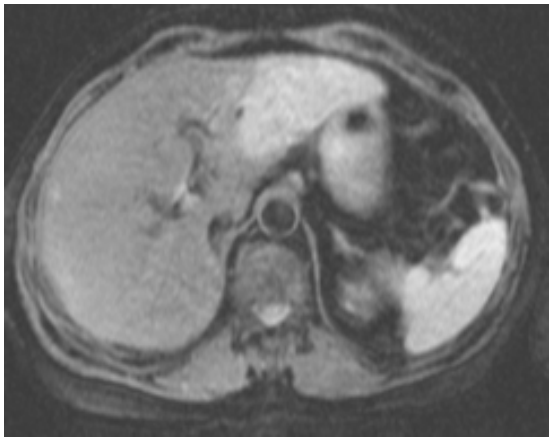

3b.

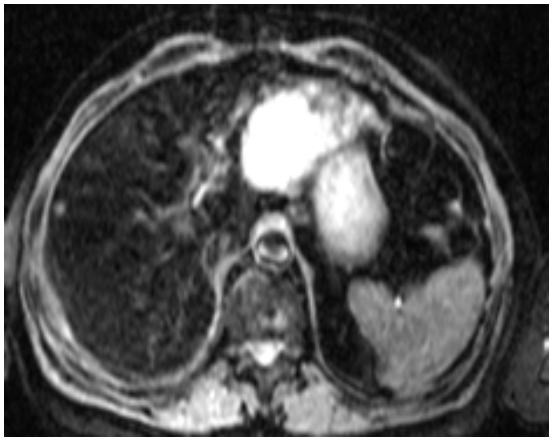

Figures 4a and b. (**a**) Unenhanced STIR image reveals a dorsally located hyperintense lesion in the right liver lobe. (**b**) SPIO-enhancement renders the lesion more conspicuous due to the signal blackening of the surrounding liver. At operation, the lesion proved to a metastasis from colon carcinoma.

4a.

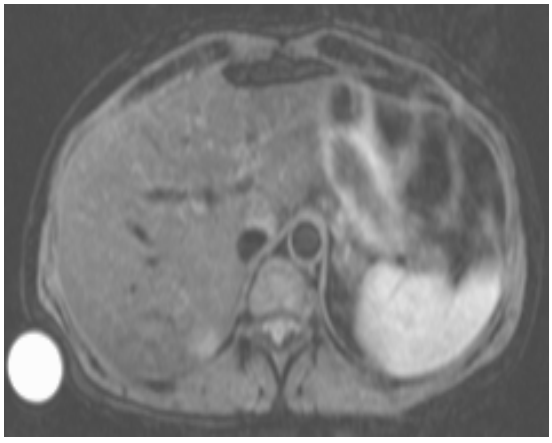

4b.

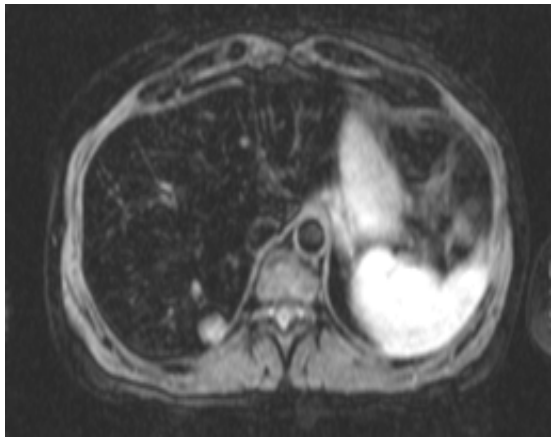

Table 1. The SNR values from liver parenchyma and liver tumors in the unenhanced and SPIO-enhanced images (values are mean±1SD).

Sequence	Liver	Tumor
T1W unenhanced	45±18	36±21
T1W SPIO-enhanced	24±10	39±20
PDW unenhanced	45±14	47±20
PDW SPIO-enhanced	19±7	38±14
T2W unenhanced	15±5	32±11
T2W SPIO-enhanced	3±1	27±9
STIR unenhanced	21±8	34±14
STIR SPIO-enhanced	6±3	31±14

Table 2. The contrast-to-noise (CNR) ratios of the liver tumors in the unenhanced and SPIO-enhanced images (values are mean±SD).

Sequence	Tumor CNR
T1W unenhanced	6±12
T1W SPIO-enhanced	15±13
PDW unenhanced	2±10
PDW SPIO-enhanced	18±10
T2W unenhanced	16±10
T2W SPIO-enhanced	24±9
STIR unenhanced	14±8
STIR SPIO-enhanced	25±13

4. Manganese Dipyridoxyl-Diphosphate (IV)

After MnDPDP administration, the T1-weighted sequences demonstrated positive parenchymal enhancements of 25.3±9.7% and 33.6±2.7% (mean±1SEM) for the SE and GE sequences, respectively. With the STIR sequence, the detected signal decrease (negative enhancement) in the liver parenchyma was 78.9±2.1% (mean±1SEM). The liver lesions demonstrated also slight enhancement with MnDPDP with mean 19.9% and 15.6% signal increases with the T1-weighted SE and GE sequences, respectively, and a mean signal drop of 5.5% by using the STIR sequence.

The calculated CNR values for liver lesions in the pre- and postcontrast images are presented in **Table 3**. For all sequences, MnDPDP-enhanced images demonstrated significantly higher CNR values when compared with their precontrast counterparts ($p=0.017$, $p=0.0001$, and $p=0.0001$, for the T1-weighted SE and GE sequences, and the STIR sequence, respectively). The STIR sequence produced the highest increase in CNR (149.0±25.5%, mean±1SEM), whereas the CNR increased by 58.5±12.7% and by 83.3±7.2% with the T1-weighted SE and GE sequences, respectively. Of the nonenhanced sequences, the T2-weighted SE sequence showed the highest mean CNR value (17.1), but it was significantly inferior when compared to the MnDPDP-enhanced STIR (mean CNR=30.3, $p=0.0001$) or T1-weighted GE sequence (mean CNR=21.3, $p=0.026$).

MnDPDP increased the number of detected lesions (**Table 4**). The highest number of lesions was found with the MnDPDP-enhanced STIR sequence (58 lesions). The greatest gain in lesion count from pre- to postcontrast images was seen in the used T1-weighted GE sequence (31.6%), while the T1-weighted SE and the STIR sequences showed increases of 24.1% and 29.0%, respectively. For all sequences, the differencies in lesion counts between the pre- and postcontrast MRI studies were statistically significant ($p<0.05$).

Table 3. The contrast-to-noise (CNR) ratios of liver tumors in the unenhanced and MnDPDP-enhanced images (absolute values, mean±1SD).

Sequence	Tumor CNR
Unenhanced T1W SE	10.3±5.5
MnDPDP-enhanced T1W SE	14.8±6.7
Unenhanced T1W GE	12.0±4.4
MnDDP-enhanced T1W GE	21.3±6.6
Unenhanced STIR	13.9±5.6
MnDPDP-enhanced STIR	30.3±9.0

Table 4. The numbers of lesions detected with different techniques.

Sequence	Unenhanced	MnDPDP-enhanced
T2W SE	32	NA
T1W SE	29	36
T1W GE	38	50
STIR	45	58

Note: NA=not assessed

Examples of MnDPDP-enhanced MR images are provided in **Figures 5 and 6**.

Figures 5a and b. (**a**) Unenhanced T1-weighted GE image demostrates a hypointense lesion in the right liver lobe, and some vague hypointensity in the caudate lobe as well. (**b**) In the MnDPDP-enhanced image these lesions are more readily detectable. Colon carcinoma metastases were found at surgery.

5a.

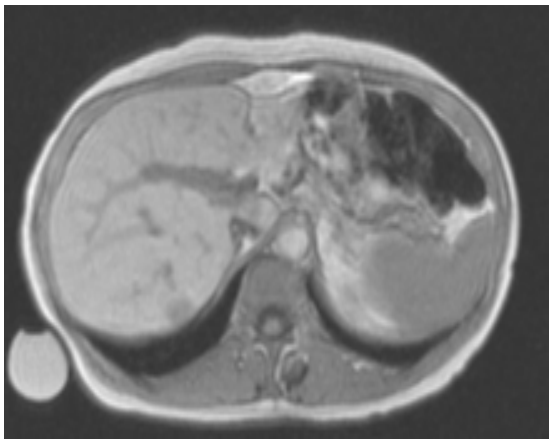

5b.

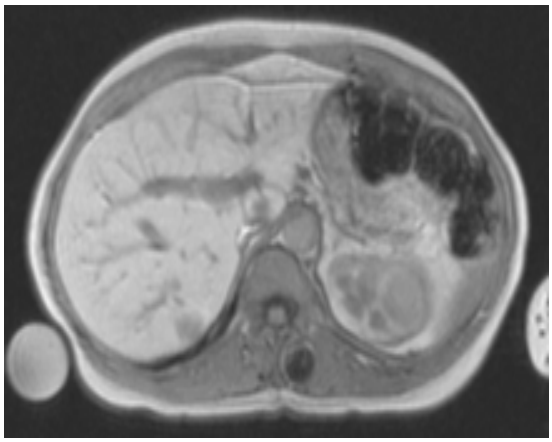

Figures 6a and b. (**a**) In this STIR image, a large and relatively homogeneously hyperintense mass lesion is seen in the right liver lobe. (**b**) In the MnDPDP-enhanced STIR image the same lesion in barely visible. The finding suggests MnDPDP-uptake of the lesion and thus, a tumor of hepatocellular origin. At surgery, a well-differentiated hepatocellular carcinoma was found.

6a.

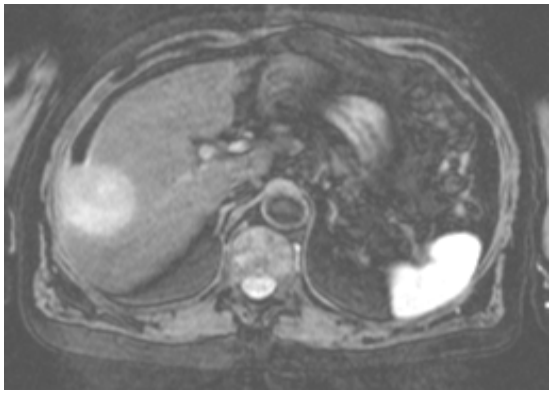

6b.

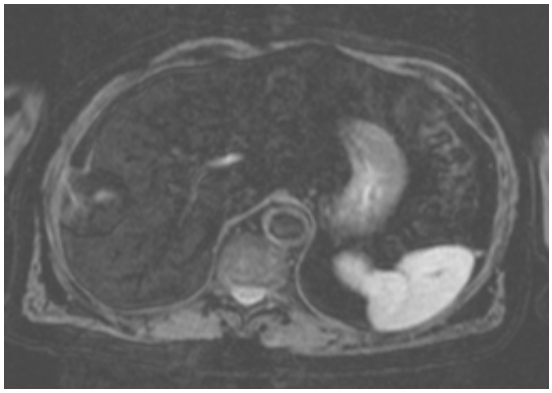

5. Combined Use of Superparamagnetic Iron Oxide and Gadolinium (V)

The numbers of liver lesions and the respective sensitivities with sequence-by-sequence basis are presented in **Table 5**. SPIO-enhanced imaging showed the greatest number of lesions (n=58, 95% sensitivity). Unenhanced MRI demonstrated 55 lesions (90% sensitivity). Gadolinium-enhanced MRI with fatsuppressed T1-weighted sequence with or without SPIO was clearly inferior with lesion counts of 49 and 47, respectively. The combined use of gadolinium and SPIO showed only two additional lesion not seen in gadolinium-enhanced images.

From single sequences, the best performance was seen with the SPIO-enhanced fast spin-echo (fSE) STIR (TR/TE/TI=3250/85/180 ms, respectively) sequence which detected 56 of the 61 lesions (92% sensitivity). Unenhanced fSE STIR and SPIO-enhanced fatsuppressed T2-weighted techniques had sensitivities of 89% and 90%, respectively. SPIO-enhancement did not significantly increase the number of detected lesions with any sequence except with the True FISP technique ($p<0.05$) which demonstrated an increase of 15% in lesion count (43 and 51 lesions in the nonenhanced and SPIO-enhanced techniques, respectively). The SPIO-enhanced True FISP sequence had a sensitivity of 84% for lesion detection.

Table 5. The numbers of focal liver lesions with different techniques. The sensitivities (in %) are shown in brackets. The sensitivities are calculated assuming that the overall lesion count is 61.

Sequence	Unenhanced	Gd	SPIO	SPIO and Gd
True FISP	43 (70)	NA	51 (84)	NA
fatsuppressed T2	52 (85)	NA	55 (90)	NA
fatsuppressed T1	42 (69)	47 (77)	42 (69)	49 (80)
fast-SE STIR	54 (89)	NA	56 (92)	NA
Total count	55 (90)	47 (77)	58 (95)	49 (80)

Note: NA=not applicable

DISCUSSION

Focal hepatic lesions are commonly discovered during routine radiological examinations. Not only the detection of metastases, but also the determination of their number are important when cancer patients, especially those with colorectal malignancies, are evaluated. Additionally, it is essential to distinguish a benign hepatic lesion from a malignant one because of their different clinical implications. Current improvements in liver surgery, and local invasive therapies with a curative potential put imaging into highlight when evaluating patients with liver metastases. Liver tumor imaging beholds two equally important tasks: there is a need for effective lesion detection (high sensitivity), and a desire for accurate tumor characterization (high specificity).

The radiology of liver tumors has gone through a radical change over the last decade with the introduction of abdominal MRI, and with the development of new CT techniques such as multidetector systems. MRI is currently considered to be the most accurate noninvasive method in the evaluation of liver lesions (Semelka et al., 1997; Reimer at al., 2000). The utilization of tissue-specific contrast agents such as SPIO or MnDPDP, and the possibility to employ MR techniques that alter tissue-contrast such as MT and the multiple slice SL render MRI an attractive tool for liver imaging.

1. Lesion Characterization

In MR imaging, multiple sequences are required for accurate lesion characterization. A magnitude of research has been focused on finding methods for reliable differentiation between various liver foci. Nevertheless, liver biopsy is still sometimes warranted, especially if surgery is planned.

In the early days of clinical liver MRI, T2 relaxation time differencies (Ohtomo et al., 1985; Goldberg et al., 1991) or differencies in the SIR (Egglin et al., 1990; Itoh et al., 1990) were thought to resolve the problem of the differentiation between malignant and benign lesions. Later, at 1.5T the difference in T2 relaxation rate with a 112ms cutoff value was found to yield a 92% sensitivity, and an accuracy of 97% in the discrimination of hemangiomas and malignant liver tumors (McFarland et al., 1994). Goldberg et al. found no overlap in the T2-values between hemangiomas and metastases

with ultrafast MR imaging (Goldberg et al., 1998). Tang et al. detected the CNR values of hemangiomas and cysts to be significantly higher than those of metastases with no overlap (Tang et al., 1998). Additionally, a variety of different MR features such as lesion signal characteristics (Brown et al., 1991; Tang et al., 1998) or contrast uptake patterns (Mathieu et al., 1991; Mitchell et al., 1994) have also been proposed in the lesion differentiation.

1.1 Multiple slice spin lock technique

MT has shown potential in the discrimination between benign and malignant liver lesions (Outwater et al., 1992; Loesberg et al., 1993). We detected similar results with the use of the multiple slice SL technique. The SL-effects from normal liver and liver metastases were nearly equal. However, the measured SL-effects from normal liver parenchyma, hemangiomas and hepatic metastases were greater when compared to the respective MT-effects. Furthermore, there was a definite difference between the MT- and SL-effects obtained from hemangiomas. Our results suggest that, in a low-field environment, the multiple slice SL technique can be used in the differential diagnosis between hemangiomas and metastases similarly to MT, but the SL technique is more efficient in generating MT-like tissue contrast than conventional MT based sequence. Additionally, with the SL technique T1□ dispersion studies can be performed (Lamminen et al., 1993; Markkola et al., 1996). Therefore, it may be assumed that the multiple slice SL technique may provide better potential for tissue characterization than the MT technique in liver tumor imaging.

In our studies with the multiple slice SL technique, there was little overlap in the SL-effects between the hemangiomas and metastases (Figure 1.). With a SL-effect cut-off value of 0.5, the distinction between hemangiomas and metastases could be made with a 91% diagnostic accuracy. With the MT technique, the overlap was greater (Figure 2.) and the diagnostic accuracy lower (85%). Our results with the multiple slice SL technique at 0.1T are comparable with previous studies that were conducted at high magnetic field strengths (Itai et al., 1985; Ohtomo et al., 1985; McFarland et al., 1994). It may be assumed that the utilization of T1 relaxation at a very low field strength with the SL technique (T1ρ relaxation) contributes to the differentiation of macromolecular tissue (metastases) and blood-containing spaces (hemangiomas), as macromolecule-water interactions are better observed at very low field strengths. Also, the differencies in proton T1 relaxation rates between blood and liver tissue increase when the effective field strength is 0.1T or lower (Koenig et al., 1984).

Our multiple slice SL studies were performed at 0.1T field-strength. It may be assumed that the favourable results thus obtained could be further improved in higher field strengths with higher SNRs. At 0.1T, specific absorption rate (SAR) was not a problem (0.084 W/kg). Because SL technique utilizes short pulses, it may be expected that SAR would not limit the use of SL in higher fields.

1.2 Superparamagnetic iron oxide and manganese dipyridoxyl-dophosphate

Hahn et al. have reported that by using SPIO, postcontrast lesion signal reductions of over 40% are characteristic for benign lesions (Hahn et al., 1992). It has been shown that FNH demonstrates uptake of SPIO (Precetti-Morel et al., 1999; Paley et al., 2000). In our series with SPIO, two hemangiomas and one FNH were included. In our solitary case of FNH, the reduction in lesion signal intensity in the T2-weighted SE (TR/TE =1900/90 ms) images was 36%, and the decrease was 59% by using the STIR sequence (TR/TE/TI=1900/20/150 ms). With two hemangiomas, similar findings were detected. In our study population, malignant liver foci did not demonstrate significant changes in signal intensities.

The accumulation of MnDPDP in liver lesions of hepatocellular origin is well-documented (Ni et al., 1993; Rofsky et al., 1993; Coffin et al., 1999). This may serve as a basis for lesion characterization. In our series with MnDPDP, we included one case of histologically verified well-differentiated HCC. This lesion demonstrated considerable contrast uptake with signal intensity increase of 50% in both SE (TR/TE=600/17 ms) and GE (TR/TE=153/6 ms) T1-weighted images, and a signal reduction of 69% in the STIR (TR/TE/TI=1900/20/150 ms) images. However, hepatic metastases from endocrine cancers have also demonstrated MnDPDP-uptake (Wang et al., 1998).

2. Lesion Detection

Numerous investigations have been conducted to compare the sensitivities of different imaging techniques in the detection of liver tumors (Rummeny et al., 1992; Ohlsson et al., 1993; Semelka et al., 1999). Research has been devoted to improve the effectiveness of any technique to increase the detection rate. In MRI, the use of various contrast agents has been the focus over the past decade.

2.1 Superparamagnetic iron oxide

CNR values reflect lesion conspicuity (Tsang et al., 1988). The higher the CNR, the more readily detectable the lesion is. Therefore, it may be considered as a measure of the effectiveness of a pulse sequence in lesion detection. Multiple reports have shown that CNR is improved by SPIO administration and thus, more lesions are detected (Fretz et al., 1990; Bellin et al., 1994; Oudkerk et al., 1997). Moreover, it has been shown that SPIO-enhanced MRI is superior to unenhanced MRI or contrast-enhanced CT in lesion detection (Lencioni et al., 1998; Hammerstingl et al., 1999; Müller et al., 1999; Poeckler-Schoeniger et al., 1999; Schultz et al., 1999; Reimer et al., 2000; Ward et al., 2000). SPIO increases the detection rate of focal lesions with cirrhotic patients (Hammerstingl et al., 2000). Our results with SPIO are in agreement with earlier studies, and investigations performed afterwards. The signal intensities obtained from normal liver parenchyma were significantly lower in the postcontrast images with all used pulse sequences. The greatest effect was seen with the T2-weighted SE sequence with signal reduction of 78%. Because SPIO had only slight effects on the signal intensity of the malignant lesions, the CNR values of liver lesions were significantly increased with all pulse sequences. Hence, postcontrast MRI demonstrated considerably greater number of lesions than the precontrast studies (n=106 and 81, respectively). Additionally, greater number of small lesions under 1 cm in diameter was detected (n=59 and 46, respectively).

As seen from our study III and supported by literature, at field-strengths of 1.0T or lower, SPIO clearly depicts a greater number of lesions than seen in plain images (Fretz et al., 1990; Seneterre et al., 1996; Ward et al., 2000). Contradictory reports, however, are available (Marchal et al., 1989; Denys et al., 1994; Duda et al., 1994). In our study at 1.5T (V), SPIO slightly increased the number of detected liver lesions but no statistical difference could be established (p=0.77). However, the highest number of lesions was seen with SPIO-enhanced imaging.

2.2 Manganese dipyridoxyl-diphosphate

There are several investigations demonstrating the efficacy of MnDPDP in liver tumor MRI (Young et al., 1990; Hamm et al., 1992; Aicher et al., 1993; Federle et al., 2000b). MnDPDP is considered to be a T1-contrast agent, and it has been found more effective in conjunction with T1-weighted GE sequences when compared with SE techniques (Wang, 1998). With the imaging parameters we used, our findings are in accordance with mean liver signal enhancements of 33.6% and 25.3% with

the use of GE (TR/TE=153/6 ms) and SE (TR/TE=600/17 ms) sequences, respectively. This allowed us to detect significantly ($p<0.05$) greater number of lesions with the T1-weighted GE sequence (n=50) when compared with the SE technique (n=36). We believe that this difference may partly be explained with the fact that the GE sequence used in our study was a breathhold sequence thus reducing the movement artefacts. However, with both T1-weighted sequences, the number of detected liver lesions was significantly greater with the MnDPDP-enhanced imaging than with the non-enhanced studies ($p<0.05$).

The hepatic enhancement with MnDPDP has demonstrated variability. An experimental dose of 50 µmol/kg MnDPDP with T1-weighted sequences at 1.5T resulted in hepatic enhancement of up to 105% (Young et al., 1990). Marchal et al. detected mean relative enhancement of 52.5% with a dose of 0.025 mmol/kg at 1.0T (Marchal et al., 1993). We observed a mean hepatic enhancement with the T1-weighted SE and GE sequences of 25.3% and 33.6%, respectively. This is less than previously reported. Our finding may have several explanations. First, the sensitivity of a T1-weighted MR sequence for paramagnetic contrast agents is related to field strength as previously shown with gadopentetate dimeglumine (Chang et al., 1994). MnDPDP studies have been performed at different field strengths ranging from 1.0T to 1.5T. Our study was conducted at 1.0T resulting to less enhancement than at 1.5T. Secondly, Liou et al. demonstrated that the lower the administered dose of MnDPDP, the less enhancement is observed (Liou et al., 1993). We used a patient dose of 5 µmol/kg while doses of 8, 12, or even 50 µmol/kg have been used in previous studies with greater enhancement values. Finally, our T1-weighted SE sequence with a TR=600ms and TE=17ms was not as strongly T1-weighted as those used by other investigators.

The combined capability of accurate lesion detection and potential to lesion characterization renders MnDPDP an attractive method to evaluate patients with known hepatic tumors.

2.3 The short inversion time inversion recovery sequence

The STIR sequence was introduced to clinical MRI by Bydder et al. in 1985 (Bydder et al., 1985a; Bydder et al., 1985b). The technique has been found to be sensitive in the detection of abdominal

malignancies, and other pathological processes in tissues (Dwyer et al., 1988; Lamminen et al., 1994). However, there are few reports available of the use of the STIR technique in conjunction with liver-specific contrast agents such as SPIO and MnDPDP. In a study performed at 0.6T, Fretz et al. found the STIR sequence to have low SNR and CNR, with and without the use of a contrast medium (Fretz et al., 1989). However, with the parameters used in our study at 1.0T with SPIO, the CNR obtained with the STIR technique was the highest of all contrast-enhanced sequences, and measured contrast enhancement was second only to the T2-weighted SE sequence. The difference in results might be explained by the different field strenght and different imaging parameters. Moreover, we used presaturation pulses to reduce motion artifacts also with the STIR sequence, which is not reported in their study.

From our results can be concluded that it is feasible to suppress signal in MnDPDP-enhanced liver tissue with the use of the STIR sequence. The number of detected lesions was superior to other sequences with or without MnDPDP-enhancement. Negative hepatic enhancement was markedly greater with the STIR technique than the positive enhancement obtained with either of the T1-weighted sequences. MnDPDP-enhanced STIR imaging displayed significantly higher lesion-to-liver CNR values than any other sequence. Our findings are supported by experimental data from Mühler et al (Mühler et al., 1992). Their investigation demonstrated the effectiveness of an experimental hepatocyte-targeted paramagnetic gadolinium chelate Gd-EOB-DTPA in the MR imaging of focal liver lesions in rats. By utilizing the STIR sequence at 2.0T with Gd-EOB-DTPA, Mühler and his colleagues achieved a negative hepatic enhancement of more than 80%. With MnDPDP, we measured a mean signal decrease of 79% by using the STIR sequence. The signal decline of MnDPDP-enhanced hepatic parenchyma in the STIR images can be explained with the increased relaxation rate. The value of the null point (intercept of the T1 relaxation curve and the T1 axis) for the T1 relaxation curve of MnDPDP-enhanced liver parenchyma approaches the null point of fat tissue.

2.4 Combined use of superparamagnetic iron oxide and gadolinium

Although Gd-enhanced T1-weighted sequences are beneficial in the characterization of liver lesions (Hamm et al., 1994; Mahfouz et al., 1994), they have only negligible effect on the detection rate (Hamm et al., 1992). On the other hand, SPIO is primarily a T2-contrast agent, and has little

contribution on the conspicuity of hepatic lesions in T1-weighted images. The results of our double contrast investigation (V) indicate that the simultaneous use of SPIO and gadolinium does not increase the effectiveness of liver MRI. Only two additional lesions were detected with combined use of SPIO and Gd-DOTA by using fatsuppressed T1-weighted SE (TR/TE=85.6/4.1 ms) sequence when compared with only Gd-enhanced imaging (Table 5).

T2-weighted sequences are considered to be the most sensitive techniques in the MRI of liver tumors (Rummeny et al., 1992). Our results in study V are in agreement with these previous findings. Unenhanced fatsuppressed T2-weighted gradient echo sequence (Half-Fourier Acquisition Single-shot Turbo spin-Echo, HASTE) (TR/TE=4.2/59 ms) demonstrated the second greatest number of lesions among the unenhanced sequences (n=52, 85% sensitivity). SPIO-enhancement slightly increased the lesion count (n=55, 90% sensitivity). The best performance (n=56, 92% sensitivity) was achieved with the SPIO-enhanced fast SE-STIR sequence (TR/TE/TI=3250/85/180 ms). The STIR technique has previously been been shown to be highly sensitive to pathological conditions such as liver tumors (Paulson et al., 1994) and our results agree with the these findings.

With fatsuppressed T2-weighted sequence, all image information is acquired after a single excitation pulse, which is followed by a long train of refocusing RF-pulses. Images with good resolution and with negligible motion artifacts may be obtained. With the True FISP (Fast Imaging with Steady state free Precession), the FISP and PSIF (reverse FISP) echoes are produced at the same time, so only one combined signal is received. FISP produces images with T1/T2 contrast due to the preserved transverse magnetization component and PSIF produces images with heavy T2-weighting due to the very long echo times. With fast spin echo (SE)-STIR, a train of echoes follows each excitation pulse. Fast SE-STIR requires fewer TRs and TIs to acquire a given amount of data. Therefore it is more efficient than conventional SE-STIR. With fast SE-STIR, longer effective echo times (TE_{eff}) are practical because it allows more signal averaging than conventional SE-STIR. If long TE_{eff} is used, fast SE-STIR images are heavily T2-weighted in addition to the T1 contrast inherent in STIR techniques.

According to our investigation, double-contrast MRI with SPIO and gadolinium was not beneficial. If only T1-weighted images are evaluated, Gd-enhancement increased the number of detected liver

lesion from 42 to 47. However, Gd-enhanced MRI did not reveal any additional lesions in comparison with the unenhanced T2-weighted sequence. Our finding is supported by a recent report by Hamm et al. (Hamm et al., 1997). They concluded that at 1.5T unenhanced MRI is as sensitive in the detection of liver lesions as Gd-enhanced imaging. Our results indicate that unenhanced T2-weighted sequences outnumber T1-weighted sequences either with or without gadolinium in lesion detection. Despite the negligible results, it may be assumed that double-contrast MRI with increased detection potential in conjunction with the good lesion characterization capabilities of the contrast agents renders the technique attractive to liver MRI. This assumption is supported by the recent investigation by Kubaska et al. (Kubaska et al., 2001) in which the good lesion characterization capability of gadolinium was shown to maintain after SPIO administration.

3. Safety of Contrast Agents

The overall rate of side-effects of gadolinium is low (Nelson et al., 1995). We did not detect any side effects with the use of Gd-DOTA.

The adverse reactions of SPIO are well established, the occurrence ranging from 6.1 to 10.3% (Laniado and Chachuat, 1995). Low back pain is the most commonly reported side-effect. In the present thesis, SPIO was administered to 40 patients. Side-effects were recorded with six patients (15%), one of them being an anaphylactic reaction which could be related to the contrast agent. Five patients complained lumbar pain.

A recent investigation reports an adverse reaction rate of 23% with the use of MnDPDP (Federle et al., 2000a). The most commonly reported adverse events were nausea and headache. The investigators state that most of these mild side-effects were not drug related and did not require treatment. The incidence of serious adverse reactions was lower (1.6%), and not drug related. In our study group of 20 patients, however, we did not detect any side-effects. The difference in adverse events may be explained with the different injection rates. Federle et al. used an injection over one minute and we administered the MnDPD-solution with an approximately 20 minute infusion.

4. Liver MRI: current trends and look into the future

Liver-specific contrast agents have definitively improved the performance of liver MRI especially when non-cirrhotic livers harboring focal lesions are in question. The contrast agent research still pursues for targeted and more effective agents with a safe profile. High-field MR systems of 1.5T have been advocated for liver MRI. Furthermore, even field strengths of 3.0T are in clinical use for neuroradiology but yet not utilized in liver MRI. With high-field MR imagers, breathhold scanning with very short TE's may be performed. Movement artefacts are essentially reduced. Higher spatial resolution is also obtained. The developments in coil technology even further increases the capabilities of MRI in the quest for effective liver tumor imaging.

Although gadolinium has shown great potential in the diagnosis of liver hemangiomas, focal nodular hyperplasias and hepatic metastases, there are still uncertainties especially when small lesions are considered. The characteristic T2-hyperintensity and Gd-enhancement patterns of hemangiomas may be similar with liver metastases especially when small lesions are concerned. The True FISP sequence has shown potential in the characterization of liver lesions demonstrating small and large liver cysts and hemangiomas as markedly bright lesions while practically all malignant liver foci appear only slightly hyperintense or isointense with respect to normal liver parenchyma.

Originally, SPIO was designed for T2-weighted MRI in order to increase the conspicuity and hence, detection rate of focal liver lesions. However, recent investigations have expanded the utility of SPIO towards the characterization of liver lesions. SPIO-enhanced MRI with the use of T1-weighted sequences has been found helpful with this respect (Kim et al., 2002). Additionally, the T1 effects of SPIO, given as a bolus for dynamic imaging, have proved to be useful in the diagnosis of liver hemangiomas (Sahani et al., 2002).

Interventional MRI is emerging (Ojala el al., 2002). In future, liver lesions with important clinical implications may be the target of MRI-guided biopsy. Magnetic resonance spectroscopy (MRS) is evolving. To date, it is valid in the evaluation of diffuse liver diseases such as fatty degeneration (Ryysy et al., 2000). Its role in focal liver lesions remains to be assessed.

Liver MRI is under a continuous progress. This means better coils, higher magnetic field strengths with the capability of motion ’freezing’, and above all, advanced techniques for increased lesion detection and improved characterization potential. The multiple slice SL technique may play a role in lesion characterization even in high magnetic field strengths because the SAR is not compromized. Liver-specific contrast agents play a special role when evaluating patients with liver lesions, especially when invasive treatment is considered.

CONCLUSIONS

1. The multiple slice SL technique provides improved tissue contrast in liver MR when compared to conventional MT imaging.

2. The multiple slice SL MR imaging technique showed high diagnostic accuracy in the differentiation of hepatic hemangiomas and liver metastases. The results were comparable or even superior to the magnetization transfer (MT) technique.

3. More lesions can be detected with superparamagnetic iron oxide (SPIO)- and manganese dipyridoxyl-diphosphate (MnDPDP)-enhanced MRI when compared with unenhanced imaging because of a considerable increase in the lesion CNR values. The short inversion time inversion recovery (STIR) sequence proved to be the most effective sequence in the lesion detection with both tissue-specific contrast agents.

4. Double contrast MRI, i.e. combined use of SPIO and Gd-DOTA, did not increase the sensitivity of lesion detection at 1.5T. The fast SE-STIR sequence demonstrated the best performance in this investigation (V).

SUMMARY

Imaging of liver diseases, especially focal liver lesions, has progressed enormously with the development of MRI technology and contrast agents. Modern MRI with update sequences and contrast agents is noninvasive and highly accurate in examining patients with known or suspected liver lesions, even at low-field strengths. Our results demonstrated that the lesion characterization potential of the multiple slice spin lock (SL) technique at 0.1T was comparable to investigations performed at considerably higher field strengths.

The multiple slice SL technique provides tissue contrast characteristics similar to that of the magnetization transfer (MT) technique. However, the ability in tissue discrimination facilitated by the locking pulse taking advantage of very low magnetic field strength even exceeds that of the MT technique as shown by our results. The capability of distinguishing hepatic hemangiomas and liver metastases at 0.1T gave promising results with the multiple slice SL technique. This technique may also be employed in higher magnetic field strengths.

Contrast agents provide another tool for improving the performance of MRI in liver lesion detection and characterization. Tissue-specific agents such as superparamagnetic iron oxide (SPIO) and manganese dipyridoxyl-diphosphate (MnDPDP) are specifically designed for liver lesion detection. Our studies demonstrated that the use of SPIO and MnDPDP improved lesion detection. The implementation of the STIR sequence in conjunction with these agents proved to be useful. Although these agents have provided controversial data at different MR field strenghts, their impact on lesion detection is considerable at least with field-strength of 1.0T.

Double-contrast MR imaging is emerging. The idea of differently acting contrast agents is attractive, and recent literature has provided encouraging results. Our results at 1.5T with superparamagnetic iron oxide (SPIO) and gadolinium were negligible when lesion detection is considered. The discrepancy between earlier studies and our results may be due to different patient population. We included only non-cirrhotic patients while cirrhotic patiens have been evaluated earlier. Therefore it may be assumed that in the future, double-contrast liver MRI may play an important role in the further evaluation of patients with liver lesions.

In conclusion, the studies included in the present thesis have demonstrated the feasibility of contrast modifying techniques in the detection and characterization of liver lesions. The combined use of SPIO and gadolinium at 1.5T proved to be of negligible benefit in the detection of liver lesions.

ACKNOWLEDGMENTS

This study was carried out at the Department of Radiology, Helsinki Central University Hospital, during the years 1992-1999.

I would like to express my gratitude to the Professor of Diagnostic Radiology, Carl-Gustaf Standertskjöld-Nordenstam, M.D., for his interest towards my work and for providing the excellent MRI units at my disposal. I also wish to thank Professor Ilkka Suramo, M.D., for introducing me the idea of investigating liver MRI.

Docent Sören Bondestam, M.D., has been my supervisor with remarkable patience during the long years of preparation of this thesis. His excellence and wisdom in scientific work have been of great significance. I'm sincerely in great debt to him.

I wish to thank all my co-authors. The tremendous help and guidance from Docent Antti Lamminen, M.D., was paramount. The friendship of Dr. Pekka Tervahartiala, M.D., has meant a lot to me. Above all, I would like to express my deepest gratitude to Professor Raimo Sepponen, Ph.D., for providing his expertise in MR technology at my disposal, and for introducing me the enchanting world of multiple slice SL MR imaging. Despite of his (hundreds of) other activities, he was able to spare a few minutes every now and then for my purposes in order to complete a manuscript or design new investigations.

I wish to thank the official reviewers, Professor Sanjay Saini, M.D. Ph.D., Massachusetts General Hospital and Harvard Medical School, and Docent Pekka Niemi, M.D., University of Turku, for their positive attitude towards the revision of the manuscript. I obtained many valuable comments and constructive criticism from their thorough evaluation of the manuscript.

I have the honor to express my very special thanks and deep admiration to the four Docents: Juhani Rauste, M.D., taught me the basics of radiology a long time ago at Jorvi Hospital. I still carry the memories in my heart with great respect. Juhani means a lot to me, and not only professionally. Pauli Hekali, M.D., is a special guy. Pauli is a tremendeous radiologist and a friend. I truly respect his attitude towards colleagues and other hospital personnel not to mention the patients. For some reason, he showed interest toward my thesis. There were times I did not welcome his questioning!

Kalevi Somer, M.D., is a corner-stone to my profession. Kalevi's humble and caretaking attitude toward younger radiologists was outstanding. I felt comfortable with him. After coming back from the U.S.A in 1996, I started to collaborate with Hannu Suoranta , M.D., both professionally and academically. Either way, I admire the expertise he continuously demonstrates. To my delight, Hannu has achieved a more pronounced title as we are speaking. I sincerely congratulate him!

My warmest thanks are due to the personnel of the Department of Radiology. I would like to express my special thanks to the staff of the MRI unit. Maire Engman was helpful and patient with me. MR technologists showed competence in performing contrast-enhanced liver MRI. Even though the MR imaging sessions were sometimes strenuous, we all had fun and learned a lot. My colleagues at the Department of Neuroradiology deserve a special thanks. Antti Brander, M.D., taught me how to be humble, and how to acknowledge all the mistakes we all inevitably do as radiologists. I admire his sarcastic humor, and his interest to Pahkasika.

The personnel at the 'RTG 3' at our department is very special to me. Otherwise I guess, I wouldn't have enjoyed myself so much at Meilahti for nearly 13 years. At work the spirit of RTG3 is awesome, not to mention our sparetime activities. Docent Pekka Keto, M.D., was in duty when the honorable Society of Rail-Road Radiologists was initiated. All in all, I have had the honor to work with the very best people at the Department of Radiology.

During the preparation of my thesis I had the pleasant opportunity to visit the Center of Imaging and Pharmaceutical Research (CIPR) as a research fellow in Boston, U.S.A. I want to thank the staff of CIPR for making that year an unforgettable one. Gerald Wolff, M.D., was Head of CIPR, and I'm still influenced by his wisdom and enthusiasm in contrast agent research. Especially, I would like to express my deep gratitude to Leena Hamberg and George Hunter. They demonstrated a thorough and enthusiastic attitude towards scientific work. I was thrilled. Their friendship is something to charish. X-ray technician Marek Trocha became a true eternal companion, and I've had the pleasure to stay with his lovely family on several occasions while visiting Boston.

I am lucky to have a lot of good friends. I would like to thank Mikko Kallela, M.D., Jani Malmi, M.D., and Matti Pekonen, M.D., for the many good times we spent together during the medical school and thereafter. The families of Laukkarinen and Weckström are essential and important to me and my family. Arno de la Chapelle, Matti Huhtamies, Jarmo Raveala and Jan Sjöman have

been my closest friends for more than three decades, ever since the good old ‘Norssi times’. All in all, the non-academic and non-medical companionship of all my friends is beyond words. Finally, I’m honored to give my best to the legendary Kaksoiskiventie-group. Thank you all, folks!

I wish to thank my parents Aino and Paavo Halavaara for being there. Also, I am thankful for having a sister, Teija, and a little brother, Mika. Mika is an enthusiastic young M.D., and a resourceful young man with a good taste of music. My very special thanks are due to my late elder brother Kai Halavaara. His memory remains in the adorable family of his, especially in Jukka, my godson.

Last but not least: my very special, loving and caring thanks are due to my own family Sari, Johannes and Lauri. I’m grateful and lucky to have them with me. From now on, I’ll have the possibility to compensate for all the long hours I spent at the hospital and by the computer!

This work was supported by the Radiological Society of Finland and the Pehr Oscar Klingendahl Foundation.

Kauniainen, October 2002

Juha Halavaara

REFERENCES

Adzamli K, Dorshow RB, Hynes MR, Nosco DL, Adams MD. PEG-coated Mn-substituted hydroxylapatites as potential magnetic resonance contrast media for the blood pool. Acta Radiol 1997; 412(S):73-78.

Aicher KP, Laniado M, Kopp AF, Grönewäller E, Duda SH, Claussen CD. Mn-DPDP-enhanced MR imaging of malignant liver lesions: efficacy and safety in 20 patients. J Magn Reson Imaging 1993; 3:731-737.

Arakawa M, Kage M, Sugihara S, Nakashima T, Suenaga M, Okuda K. Emergence of malignant lesions within an adenomatous hyperplastic nodule in a cirrhotic liver. Observations in five cases. Gastroenterology 1986; 91:198-208.

Arrivé L, Flejou J-F, Vilgrain V, Belghiti J, Najmark D, Zins M, Menu Y, Tubiana JM, Nahum H. Hepatic adenoma: MR findings in 51 pathologically proved lesions. Radiology 1994; 193:507-512.

Aronen HJ, Abo Ramadan U, Peltonen TK, Markkola AT, Tanttu JI, Jääskeläinen J, Häkkinen A-J, Sepponen R. 3D spin-lock imaging of human gliomas. Magn Reson Imaging 1999; 17:1001-1010.

Atkinson D, Brant-Zawadski M, Gillan G, Purdy D, Laub G. Improved MR angiography: magnetization transfer suppression with variable flip angle excitation and increased resolution. Radiology 1994; 190:890-894.

Atlas SW, Grossman RI, Hackney DB, Goldberg HI, Bilaniuk LT, Zimmerman RA. STIR MR imaging of the orbit. Am J Roentgenol 1988; 151:1025-1030.

Baker ME, Pelley R. Hepatic metastases: basic principles and implications for radiologists. Radiology 1995; 197:329-337.

Bean CP, Livingstone JD. Superparamagnetism. J Appl Physics 1959; 30:120S.

Bellin M-F, Zaim S, Auberton E, Sarfati G, Duron J-J, Khayat D, Grellet J. Liver metastases: safety and efficacy of detection with superparamagnetic iron oxide in MR imaging. Radiology 1994; 193:657-663.

Berman MA, Burnham JA, Sheahan DG. Fibrolamellar carcinoma of the liver: an immunohistochemical study of 19 cases and a review of the literature. Hum Pathol 1998; 19:784-794.

Bernardino ME, Young SW, Lee JKT, Weinreb JC. Hepatic MR imaging with MnDPDP: safety, image quality, and sensitivity. Radiology 1992; 183:53-58.

Bottomley PA, Hardy CJ, Argersinger RE. The field dependence on T1 contrast between normal and pathologic tissue: a review (abstr.). In: Book of Abstracts: Society of Magnetic Resonance In Medicine 1986. Vol 2. Berkeley, Calif: Society of Magnetic Resonance in Medicine, 1986; 407-408.

Bottomley PA, Foster TH, Argersinger RE, Pfeifer LM. A review of normal tissue hydrogen NMR relaxation times and relaxation mechanisms from 1 - 100 MHz: dependence on tissue type, NMR frequency, temperature, species, excision and age. Med Phys 1984; 11:425-448.

Brown JJ, Lee JM, Lee JKT, van Lom, KJ, Malchow SC. Focal hepatic lesions: differentiation with MR imaging at 0.5T. Radiology 1991; 179:675-679.

Buetow PC, Midkiff RB. Primary malignant neoplasms in the adult. MRI Clin N Am 1997; 5:289-318.

Bydder GM, Pennock JM, Phil M, Steiner RE, Khenia S, Payne JA, Young IR. The short TI inversion recovery sequence– an approach to MR imaging of the abdomen. Magn Reson Imaging 1985a; 3:251-254.

Bydder GM, Steiner RE, Blumgart LH, Khenia S, Young IR. MR imaging of the liver using short TI inversion recovery sequences. J Comput Assist Tomogr 1985b; 9:1084-1089.

Bydder GM, Young IR. MR imaging: clinical use of the inversion recovery sequence. J Comput Assist Tomogr 1985; 9:659-675.

Campeau NG, Johnson CD, Felmlee JP, Rydberg JN, Butts RK, Ehman RL, Riederer SJ. MR imaging of the abdomen with a phased-array multicoil: prospective clinical evaluation. Radiology 1995; 195:769-776.

Carr DH, Brown J, Bydder GM, Steiner RE, Weinmann H-J, Speck U, Hall AS, Young IR. Gadolinium-DTPA as a contrast agent in MRI: initial clinical experience in 20 patients. Am J Roentgenol 1984; 143:215-224.

Chang KH, Ra DG, Han MH, Cha SH, Kim HD, Han MC. Contrast enhancement of brain tumors at different MR field strengths: comparison of 0.5T and 2.0T. Am J Neuroradiol 1994; 15:1413-1419.

Chung KY, Mayo-Smith WW, Saini S, Rahmouni A, Golli M, Mathieu D. Hepatocellular adenoma: MR imaging features with pathologic correlation. Am J Roentgenol 1995; 165:303-308.

de Coene B, Hajnal JV, Gatehouse P, Longmore DB, White SJ, Oatridge A, Pennock JM, Young IR, Bydder GM. MR of the brain using fluid-attenuated inversion recovery (FLAIR) pulse sequences. AJNR 1992; 13:1555-1564.

Coffin CM, Diche T, Mahfouz A, Alexandre M, Caseiro-Alves F, Rahmouni A, Vasile N, Mathieu D. Benign and malignant hepatocellular tumors: evaluation of tumoral enhancement after mangafodipir trisodium injection on MR imaging. Eur Radiol 1999; 9:444-449.

Denys A, Arrive L, Servois V, Dubray B, Najmark D, Sibert A, Menu Y. Hepatic tumors: detection and characterization at 1-T MR imaging enhanced with AMI-25. Radiology 1994; 193:665-669.

Doyle FH, Pennock JM, Banks LM, McDonnel MJ, Bydder GM, Steiner RE, Young IR, Clarke GJ, Pasmore T, Gilderdale DJ. Nuclear magnetic resonance imaging of the liver: initial experience. Am J Roentgenol 1982; 138:193-200.

Duda SH, Laniado M, Kopp AF, Grönewäller E, Aicher KP, Pavone P, Jehle E, Claussen CD. MR-tomographie fokaler leberläsionen mit dem superparamagnetischen kontrastmittel AMI-25 bei 1,5 Tesla. Fortschr Röntgenstr 1994; 160:46-51.

Dwyer AJ, Frank JA, Sank VJ, Reinig JW, Hickey AM, Doppman JL. Short-TI inversion-recovery pulse sequence: analysis and initial experience in cancer imaging. Radiology 1988; 168:827-836.

Ebara M, Ohto M, Watanabe Y, Kimura K, Saisho H, Tsuchiya Y, Okuda K, Arimizu N, Kondo F, Ikehira H. Diagnosis of small hepatocellular carcinoma: correlation of MR imaging and tumor histologic studies. Radiology 1986; 159:371-377.

Ebara M, Watanabe S, Kita K, Yoshikawa M, Sugiura N, Ohto M, Kondo F, Kondo Y. MR imaging of small hepatocellular carcinoma: effect of intratumoral copper content on signal intensity. Radiology 1991; 180:617-621.

Egglin TK, Rummeny E, Stark DD, Wittenberg J, Saini S, Ferrucci JT. Hepatic tumors: quantitative tissue characterization with MR imaging. Radiology 1990; 176:107-110.

Elizondo G, Fretz CJ, Stark DD, Rocklage SM, Quay SC, Worah D, Tsang Y-M, Chia-Mei Chen M, Ferrucci JT. Preclinical evaluation of MnDPDP: new paramagnetic hepatobiliary contrast agent for MR imaging. Radiology 1991; 178:73-78.

Engelhardt RT and Johnson GA. T1ρ relaxation and its application to MR histology. Magn Reson Med 1996; 35:781-786.

Federle M, Chezmar J, Rubin DL, et al. Efficacy and safety of mangafodipir trisodium (MnDPDP) injection for hepatic MRI in adults: results of the U.S. multicenter phase III clinical trials. (Safety). J Magn Reson Imaging 2000a; 12:186-197.

Federle M, Chezmar J, Rubin DL, et al. Efficacy and safety of mangafodipir trisodium (MnDPDP) injection for hepatic MRI in adults: results of the U.S. multicenter phase III clinical trials. Efficacy of early imaging. J Magn Reson Imaging 2000b; 12:689-701.

Finelli DA, Hurst GC, Karaman BA, Simon JE, Duerk JL, Bellon EM. Use of magnetization transfer for improved contrast on gradient echo MR images of the cervical spine. Radiology 1994; 193:165-171.

Foley WD, Kneeland JB, Cates JD, Kellman GM, Lawson TL, Middleton WD, Hendrick RE. Contrast optimization for the detection of focal hepatic lesions by MR imaging at 1.5T. Am J Roentgenol 1987; 149:1155-1160.

Fong Y, Cohen AM, Fortner JG, Enker WE, Turnbull AD, Coit DG, Marrero AM, Prasad M, Blumgart LH, Brennan MF. Liver resection for colorectal metastases. J Clin Oncol 1997; 15:938-946.

Fretz CJ, Elizondo G, Weissleder R, Hahn PF, Stark DD, Ferrucci JT Jr. Superparamagnetic ironoxide-enhanced MR imaging: pulse sequence optimization for detection of liver cancer. Radiology 1989; 172:393-397.

Fretz CJ, Stark DD, Metz CE, Elizondo G, Weissleder R, Shen J-H, Wittenberg J, Simeone J, Ferrucci JT. Detection of hepatic metastases: comparison of contrast-enhanced CT, unenhanced MR imaging, and iron oxide-enhanced MR imaging. Am J Roentgenol 1990; 155:763-770.

Gazelle GS, Goldberg SH, Solbiati L, Livraghi T. Tumor ablation with radiofrequency energy. Radiology 2000; 217:633-646.

Gehl HB, Vorwerk D, Klose KC, Gunther RW. Pancreatic enhancement after after low-dose infusion of Mn-DPDP. Radiology 1991; 180:337-339.

Gillis P, Koenig S. Transverse relaxation of solvent protons induced by magnetized spheres: application to ferritin, erythrocytes and magnetite. Magn Reson Med 1987; 5:323-345.

Goldberg MA, Saini S, Hahn PF, Egglin TK, Mueller PR. Differentiation between hemangiomas and metastases of the liver with ultrafast MR imaging: preliminary results with T2 calculations. Am J Roentgenol 1991; 157:727-730.

Gordon SC, Reddy KR, Livingstone AS, Jeffers LJ, Schiff ER. Resolution of a contraceptive-steroid-induced hepatic adenoma with subsequent evolution into hepatocellular carcinoma. Ann Intern Med 1986; 105:547-549.

Grad J, Bryant RG. Nuclear magnetic cross-relaxation spectroscopy. J Magn Reson Imaging 1990; 90:1-8.

Grad J, Mendelson D, Hyder F, Bryant RG. Direct measurements of longitudinal relaxation and magnetization transfer in heterogenous systems. J Magn Reson Imaging 1990; 86:416-419.

Gupta H, Weissleder R. Targeted contrast agents in MR imaging. MRI Clin N Am 1996; 4:171-184.

de Haen C, Gozzini L. Soluble-type hepatobiliary contrast agents for MR imaging. J Magn Reson Imaging 1993; 3:179-186.

Hahn PF, Stark DD, Weissleder R, Elizondo G, Saini S, Ferrucci JT. Clinical application of superparamagnetic iron oxide to MR imaging of tissue perfusion in vascular liver tumors. Radiology 1990; 174:361-366.

Hamm B, Mahfouz AE, Taupitz M, Mitchell DG, Nelson R, Halpern E, Speidel A, Wolf K-J, Saini S. Liver metastases: improved detection with dynamic gadolinium-enhanced MR imaging? Radiology 1997; 202:677-682.

Hamm B, Thoeni RF, Gould RG, Bernardino ME, Luning M, Saini S, Mahfouz AE, Taupitz M, Wolf K-J. Focal liver lesions: characterization with nonenhanced and dynamic contrast material-enhanced MR imaging. Radiology 1994; 190:417-423.

Hamm B, Vogl TJ, Branding G, Schnell B, Taupitz M, Wolf K-J, Lissner J. Focal liver lesions: MR imaging with MnDPDP-initial clinical results in 40 patients. Radiology 1992; 182:167-174.

Hammerstingl Jr RM, Schwarz WV, Soellner Jr, O, Lobeck R, Bechstein WO, Vogl TJ. MRI in liver transplantation: prospective evaluation using iron oxide-enhanced studies in comparison to clinical and histopathologic findings for the diagnosis of HCC. Radiology 2000; 213(P):170.

Hammerstingl RM, Schwenkenbecher J, Schwarz WV, Lobeck R, Bechstein WO, Vogl TJ. MRI of focal liver tumors: clinical single center outcome study in 900 patients using iron-oxide enhanced imaging. Radiology 1999; 213(P):170.

Hayes CE, Dietz MJ, King BF, Ehman RL. Pelvic imaging with phased-array coils: quantitative assessment of signal-to-noise ratio improvement. J Magn Reson Imaging 1992; 2:321-326.

van Hecke P, Marchal G, Decrop E, Baert AL. Experimental study of the pharmacokinetics and dose response of ferrite particles used as a contrast agent in MRI of the normal liver of the rabbit. Invest Radiol 1989; 24:397-399.

Henkelman RM, Huang X, Xiang Q-S, Stanisz GJ, Swanson SD, Bronskill MJ. Quantitative interpretation of magnetization transfer. Magn Reson Med 1993; 29:759-766.

Ichikawa T, Federle MP, Grazioli L, Madariaga J, Nalesnik M, Marsh W. Fibrolamellar hepatocellular carcinoma: imaging and pathologic findings in 31 recent cases. Radiology 1999; 213:352-361.

Itoh K, Saini S, Hahn PF, Imam N, Ferrucci JT. Differentiation between small hepatic hemangiomas and metastases on MR images: importance of size-specific quantitative criteria. Am J Roentgenol 1990; 155:61-66.

Johnson KM, Tao JZ, Kennan RP, Gore JC. Gadolinium-bearing red cells as blood pool MRI contrast agents. Magn Reson Med. 1998; 40:133-42.

Kadoya M, Matsui O, Takashima T, Nonomura A. Hepatocellular carcinoma: correlation of MR imaging and histopathologic findings. Radiology 1992; 183:819-825.

Kahn CE, Perera SD, Sepponen RE, Tanttu JI, Tierala EK, Lipton MJ. Magnetization transfer imaging of the abdomen at 0.1T: detection of hepatic neoplasms. Magn Reson Imaging 1993; 11:67-71.

Kajander S, Komu M, Niemi P, Kormano M. Determination of saturation transfer parameters of human tissues in vivo. Magn Reson Imaging 1996; 14:413-417.

Karhunen PJ. Benign hepatic tumors and tumor like conditions in men. J Clin Pathol 1986; 39:183-188.

Kawashima A, Suehiro S, Murayama S, Russel WJ. Focal fatty infiltration of the liver mimicking a tumor. J Comput Assist Tomogr 1986; 10:329-331.

Kelekis NL, Semelka RC, Worawattanakul S, de Lange EE, Ascher SM, Ahn ID, Reinhold C, Remer EM, Brown JJ, Bis KG, Woosley JT, Mitchell DG. Hepatocellular carcinoma in North America: a multiinstitutional study of appearance on T1-weighted, T2-weighted, and serial gadolinium-enhanced gradient-echo images. Am J Roentgenol 1998; 170:1005-1013.

Kim JH, Kim M-J, Suh SH, Chung J-J, Yoo HS, Lee JT. Characterization of focal hepatic lesions with ferumoxides-enhanced MR imaging: utility of T1-weighted spoiled gradient recalled echo images using different echo times. J Magn Reson Imaging 2002; 15:573-583.

Kim S-Y, Chung J-J, Kim M-J, Park S, Lee JT, Yoo HS. Atypical inside-out pattern of hepatic hemangiomas. Am J Roentgenol 2000; 174:1571-1574.

Kinnard MF, Alavi A, Rubin RA, Lichtenstein GR. Nuclear imaging of solid hepatic masses. Semin Roentgenol 1995; 30:375-395.

Kirchin MA, Pirovano GP, Spinazzi A. Gadobenate dimeglumine (Gd-BOPTA): an overview. Invest Radiol 1998; 33:798-809.

Koenig SH, Brown RD III, Adams D, Emerson D, Harrison CG. Magnetic field dependence of 1/T1 of protons in tissue. Invest Radiol 1984; 19:76-81.

Koenig SH, Bryant RG, Hallenga K, Jacob GS. Magentic cross-relaxation among protons in protein solutions. Biochemistry 1978; 17:4348-4358.

Koenig SH, Brown RD III, Ugolini R. A unified view of relaxation in protein solution and tissue, including hydration and magnetization transfer. Magn Reson Med 1993; 14:77-83.

Laing ADP, Gibson RN. MRI of the liver. J Magn Reson Imaging 1998; 8:337-345.

Lamminen AE, Anttila VJA, Bondestam S, Ruutu T, Ruutu PJ. Infectious liver foci in leukemia: comparison of short inversion-time inversion-recovery, T1-weighted spin-echo, and dynamic gadolinium-enhanced MR imaging. Radiology 1994; 191:539-543.

Lamminen AE, Tanttu JI, Sepponen RE, Pihko H, Korhola OA. T1ρ dispersion imaging of diseased muscle tissue. Br J Radiol 1993; 66:783-787.

Laniado M, Chachuat A. Vertraglichkeitsprofil von Endorem. Radiologe 1995; 11 (suppl.11):266-270.

Lee MJ, Hahn PF, Saini S, Mueller PR. Differential diagnosis of hyperintense liver lesions on T1-weighted MR images. Am J Roentgenol 1992; 159:1017-1020.

Lee MJ, Saini S, Compton CC, Malt RA. MR demonstration of edema adjacent to a liver metastasis: pathologic correlation. Am J Roentgenol 1991; 157:499-501.

Leese T, Farges O, Bismuth H. Liver cell adenomas: a 12-year surgical experience from a specialist hepato-biliary unit. Ann Surg 1988; 208:558-564.

Lencioni R, Donati F, Cioni D, Paolicchi A, Cicorelli A, Bartolozzi C. Detection of colorectal liver metastases: prospective comparison of unenhanced and ferumoxides-enhanced magnetic resonance imaging at 1.5T, dual-phase spiral CT, and spiral CT during arterial portography. Magn Reson Mat Physics, Biology and Medicine 1998; 7:76-87.

Lewis KH, Chezmar JL. Hepatic metastases. MRI Clin N Am 1997; 5:319-330.

Lim KO, Stark DD, Leese PT, Pfefferbaum A, Rocklage SM, Quay SC. Hepatobiliary MR imaging: first human experience with MnDPDP. Radiology 1991; 178:79-82.

Liou J, Lee JKT, Borrello JA, Brown JJ. Differentiation of hepatomas from nonhepatomatous masses: use of MnDPDP-enhanced MR images. Magn Reson Imaging 1993; 12:71-79.

Loesberg AC, Kormano M, Lipton MJ. Magnetization transfer imaging of normal and abnormal liver at 0.1T. Invest Radiol 1993; 28:726-731.

van Lom KJ, Brown JJ, Perman WH, Sandstrom JC, Lee JKT. Liver imaging at 1.5Tesla: pulse sequence optimization based on improved measurement of tissue relaxation times. Magn Reson Imaging 1991; 9:165-171.

Low RN, Francis IR, Sigeti JS, Foo TKF. Abdominal MR imaging: comparison of T2-weighted fast and conventional spin-echo, and contrast-enhanced fast multiplanar spoiled gradient-recalled imaging. Radiology 1993; 186:803-811.

Lu DS, Saini S, Hahn PF, Goldberg M, Lee MJ, Weissleder R, Gerard B, Halpern E, Cats A. T2-weighted MR imaging of the upper part of the abdomen: should fat suppression be used routinely? Am J Roentgenol 1994; 162:1095-1100.

Lundbom N. Determination of magnetization transfer contrast in tissue: an MR imaging study of brain tumors. Am J Roentgenol 1992; 159:1279-1285.

Mahfouz A-E, Hamm B. Contrast agents. MRI Clin N Am 1997; 5:223-240.

Mahfouz A-E, Hamm B, Taupitz M, Wolf K-J. Hypervascular liver lesions: differentiation of focal nodular hyperplasia from malignant tumors with dynamic gadolinium-enhanced MR imaging. Radiology 1993; 186:133-138.

Mahfouz A-E, Hamm B, Wolf K-J. Peripheral wash-out: a sign of malignancy on dynamic gadolinium-enhanced MR images of focal liver lesions. Radiology 1994; 190:49-52.

Makow LS. Magnetic resonance imaging: a brief review of image contrast. Radiol Clin N Am 1989; 27:195-218.

Marchal G, Zhang X, van Hecke P, Yu J, Baert AL. Comparison between Gd-DTPA, Gd-EOB-DTPA, and Mn-DPDP in induced HCC in rats: a correlation study of MR imaging, microangiopathy, and histology. Magn Reson Imaging 1993; 11:665-674.

Marchal G, Van Hecke P, Demaerel P, Decrop E, Kennis C, Baert AL, van der Schueren E. Detection of liver metastases with superparamagnetic iron oxide in 15 patients: results of MR imaging at 1.5T. Am J Roentgenol 1989; 152:771-775.

Marinelli ER, Neubeck R, Song B, Wagler T, Ranganathan RS, Sukumaran K, Wedeking PW, Nunn A, Runge VM, Tweedle MF. Synthesis, characterization, and imaging performance of a new class of macrocyclic hepatobiliary MR contrast agents. Invest Radiol 2000; 35:8-24.

Markkola AT, Aronen HJ, Paavonen T, Hopsu E, Sipilä LM, Tanttu JI, Sepponen RE. Spin lock and magnetization transfer imaging of head and neck tumors. Radiology 1996; 200:369-375.

Marti-Bonmati L, Casillas C, Graells M, Masia L. Atypical hepatic hemangiomas with intense arterial enhancement and early fading. Abd Imaging 1999; 24:147-152.

Mathieu D, Coffin C, Kobeiter H, Caseiro-Alves F, Mahfouz A, Rahmouni A, Diche T. Unexpected MR-T1 enhancement of endocrine liver metastases with mangafodipir. J Magn Reson Imaging 1999; 10:193-195.

Mattison GR, Glazer GM, Quint LE, Francis IR, Bree RL, Ensminger WD. MR imaging of hepatic focal nodular hyperplasia: characterization and distinction from primary malignant hepatic tumors. Am J Roentgenol 1987; 148:711-715.

McFarland EG, Mayo-Smith WW, Saini S, Hahn PF, Goldberg MA, Lee MJ. Hepatic hemangiomas and malignant tumors: improved differentiation with heavily T2-weighted conventional spin-echo MR imaging. Radiology 1994; 193:43-47.

McLarney JK, Rucker PT, Bender GN, Goodman ZD, Kashitani N, Ros PR. Fibrolamellar carcinoma of the liver: radiologic-pathologic correlation. Radiographics 1999; 19:453-471.

Mitchell DG, Outwater EK, Matteucci T, Rubin DL, Chezmar JL, Saini S. Adrenal gland enhancement at MR imaging with Mn-DPDP. Radiology 1995; 194:783-787.

Mitchell DG, Saini S, Weinreb J, De Lange EE, Runge VM, Kuhlman JE, Parisky Y, Johnson CD, Brown JJ, Schnall M. Hepatic metastases and cavernous hemangiomas: distinction with standard- and triple-dose gadoteridol-enhanced MR imaging. Radiology 1994; 193:49-57.

Mortelé KJ, Praet M, van Vlierberghe H, Kunnen M, Ros PR. CT and MR imaging findings in focal nodular hyperplasia of the liver: radiologic-pathologic correlation. Am J Roentgenol 2000; 175:687-692.

Müller R-D, Vogel K, Neumann K, Hirche H, Barkhausen J, Stöblen F, Henrich H, Langer R. SPIO-MR imaging versus double-phase spiral CT in detecting malignant lesions of the liver. Acta Radiol 1999; 40:628-635.

Mühler A, Clément O, Vexler V, Berthezéne Y, Rosenau W, Brasch RC. Hepatobiliary enhancement with Gd-EOB-DTPA: comparison of spin-echo and STIR imaging for detection of experimental liver metastases. Radiology 1992; 184:207-213.

Nakamura H, Ito N, Kotake F, Mizokami Y, Matsuoka T. Tumor-detecting capacity and clinical usefulness of SPIO-MRI in patients with hepatocellular carcinoma. J Gastroenterol 2000; 35:849-855.

Nakashima T, Okuda K, Kojiro M, Jimi A, Yamaguchi R, Sakamoto K, Ikari T. Pathology of hepatocellular carcinoma in Japan. 232 consecutive cases autopsied in ten years. Cancer 1983; 51:863-877.

Nelson RC, Chezmar JL, Newberry LB, Malko JA, Gedgaudas-McClees RK, Bernardino ME. Manganese dipyridoxyl diphosphate: effect of dose, time, and pulse sequence on hepatic enhancement in rats. Invest Radiol 1991; 26:569-573.

Nelson KL, Gifford LM, Lauber-Huber C, Gross CA, Lasser TA. Clinical safety of gadopentetate dimeglumine. Radiology 1995; 196:439-443.

Ni Y, Marchal G, Yu J, Rummeny E, Zhang X, Lodeman KP, Baert AL. Experimental liver cancers: Mn-DPDP-enhanced rims in MR-microangiographic-histologic correlation study. Radiology 1993; 188:45-51.

Niemi PT, Komu ME, Koskinen SK. Tissue-specificity of low-field-strength magnetization transfer contrast imaging. J Magn Reson Imaging 1992; 2:401-406.

Ohlsson B, Tranberg K-G, Lundstedt C, Ekberg H, Hederström E. Detection of hepatic metastases in colorectal cancer: a prospective study of laboratory and imaging methods. Eur J Surg 1993; 159:275-281.

Ohtomo K. Cirrhosis and premalignant nodules. MRI Clin N Am 1997; 5:331-346.

Ohtomo K, Itai Y, Furui S, Yashiro N, Yoshikawa K, Iio M. Hepatic tumors: differentiation by transverse relaxation time (T2) of magnetic resonance imaging. Radiology 1985; 155:421-423.

Ojala R, Sequeiros RB, Klemola R, Vahala E, Jyrkinen L, Tervonen O. MR-guided bone biopsy: preliminary report of a new guiding method. J Magn Reson Imaging 2002: 15:82-86.

Oudkerk M, van den Heuvel AG, Wielopolski PA, Schmitz PIM, Borel Rinkes IHM, Wiggers T. Hepatic lesions: detection with ferumoxide-enhanced T1-weighted MR imaging. Radiology 1997; 203:449-456.

Outwater E, Schnall MD, Braitman LE, Dinsmore BJ, Kressel HY. Magnetization transfer of hepatic lesions: evaluation of a novel contrast technique in the abdomen. Radiology 1992; 182:535-540.

Paley MR, Mergo PJ, Torres GM, Ros PR. Characterization of focal hepatic lesions with ferumoxides-enhanced T2-weighted MR imaging. Am J Roentgenol 2000; 175:159-163.

Paling MR, Abbitt PL, Mugler JP, Brookeman JR. Liver metastases: optimization of MR imaging pulse sequences at 1.0T. Radiology 1988; 167:695-699.

Paulson EK, Baker ME, Paine SS, Spritzer CE, Meyers WC. Detection of focal hepatic masses: STIR MR vs. CT during arterial portography. J Computer Assist Tomogr 1994; 18:581-587.

Paulson EK, McClellan JS, Washington K, Spritzer CE, Meyers WC, Baker ME. Hepatic adenoma: MR characteristics and correlation with pathologic findings. Am J Roentgenol 1994; 163:113-116.

Poeckler-Schoeniger C, Koepke J, Gueckel F, Sturm J, Georgi M. MRI with superparamagnetic iron oxide: efficacy in the detection and characterization of focal hepatic lesions. Magn Reson Imaging 1999; 17:383-392.

Powers C, Ros PR, Stoupis C, Johnson WK, Segel KH. Primary liver neoplasms: MR imaging with pathologic correlation. Radiographics 1994; 14:459-482.

Precetti-Morel S, Bellin MF, Ghebontni L, Zaim S, Opolon P, Poynard T, Mathurin P, Cluzel P. Focal nodular hyperplasia of the liver on ferumoxides-enhanced MR imaging: features on conventional spin-echo, fast spin-echo and gradient-echo pulse sequences. Eur Radiol 1999; 9:1535-1542.

Reimer P, Jähnke N, Fiebich M, Schima W, Deckers F, Marx C, Holzknecht N, Saini S. Hepatic lesion detection and characterization: value of nonenhanced MR imaging, superparamagnetic iron oxide-enhanced MR imaging, and spiral CT –ROC analysis. Radiology 2000; 217:152-158.

Reimer P, Weissleder R, Lee AS, Buettner S, Wittenberg J, Brady TJ. Asialoglycoprotein receptor function in benign liver disease: evaluation with MR imaging. Radiology 1991; 178:769-774.

Reimer P, Weissleder R, Lee AS, Wittenberg J, Brady TJ. Receptor imaging: application to MR imaging of liver cancer. Radiology 1990; 177:729-734.

Reinig JW, Dwyer AJ, Miller DL, Frank JA, Adams GW, Chang AE. Liver metastases: detection with MR imaging at 0.5 and 1.5T. Radiology 1989; 170:149-153.

Rinck PA, Fischer HW, vander Elst L, van Haverbecke Y, Müller R. Field-cycling relaxometry: medical applications. Radiology 1988; 168:843-849.

Rofsky NM, Earls JP. Mangafodipir trisodium injection (Mn-DPDP): a contrast agent for abdominal MR imaging. Magn Reson Imaging Clin N Am 1996; 4:73-85.

Rofsky NM, Weinreb JC, Bernardino ME, Young SW, Lee JKT, Noz ME. Hepatocellular tumors: characterization with Mn-DPDP-enhanced MR imaging. Radiology 1993; 188:53-59.

Ros P. Malignant liver tumors. In: Gore RM, Levinems, Laufer I (eds). Textbook of Gastrointestinal Radiology, WB Saunders, Philadelphia, 1994, pp:1897-1906.

Ros PR, Lubbers PR, Olmsted WW, Morillo G. Hemangioma of the liver: heterogenous appearance on T2-weighted images. Am J Roentgenol 1987; 149:1167-1170.

Rubin DL, Desser TS, Semelka R, Brown J, Nghiem HV, Stevens WR, Bluemke D, Nelson R, Fultz P, Reimer P, Ho V, Kristy RM, Pierro JA. A multicenter, randomized, double-blind study to evaluate the safety, tolerability, and efficacy of OptiMARK (gadoversetamide injection) compared with magnevist (gadopentetate dimeglumine) in patients with liver pathology: results of a phase III clinical trial. J Magn Reson Imaging 1999; 9:240-250.

Rummeny E, Ehrenheim Ch, Gehl HB, Hamm B, Laniado M, Lodeman KP, Schmiedel E, Steudel A, Vogl TG. Manganese-DPDP as a hepatobiliary contrast agent in the magnetic resonance imaging of liver tumors: results of clinical phase II trials in Germany including 141 patients. Invest Radiol 1991; 26:S142-S145.

Rummeny E, Weissleder R, Stark DD, Saini S, Compton CC, Bennett W, Hahn PF, Wittenberg J, Malt RA, Ferrucci JT. Primary liver tumors: diagnosis by MR imaging. Am J Roentgenol 1989; 152:63-72.

Rummeny EJ, Wernecke K, Saini S, Vassallo P, Wiesmann W, Oestmann JW, Kivelitz D, Reers B, Reiser MF, Peters PE. Comparison between high-field-strength MR imaging and CT for screening hepatic metastases: a receiver operating characteristic analysis. Radiology 1992; 182:879-886.

Ryysy L, Häkkinen A-M, Goto T, Vehkavaara S, Westerbacka J, Halavaara J, Yki-Järvinen H. Hepatic fat content and insulin action on free fatty acids and glucose metabolism rather than insulin absorption are associated with insulin requirements during insulin therapy in type 2 diabetic patients. Diabetes 2000; 49:749-758.

Sahani D, Saini S, Sharma R, O´Malley M, Harisinghani M, Hahn PF, Mueller PR. Characterizing liver hemangiomas on ferumoxides-enhanced dynamic T1-weighted imaging: preliminary experience. Acad Radiol 2002; 9(suppl 1):S255-S256.

Saini S, Stark DD, Hahn PF, Bousquet J-C, Introcasso J, Wittenberg J, Brady TJ, Ferrucci JT Jr. Ferrite particles: a superparamagnetic MR contrast agent for enhanced detection of liver carcinoma. Radiology 1987; 162:217-222.

Saini S, Sharma R, Baron RL, Turner DA, Ros PR, Hahn PF, Small WC, Delange EE, Stillman AE, Edelman RR, Runge VM, Outwater EK. Multicentre dose-ranging study on the efficacy of USPIO ferumoxtran-10 for liver MR imaging. Clinical Radiology 2000; 55:690-695.

Santyr GE, Fairbanks EJ, Kelcz F, Sorenson JA. Off-resonance spin locking for MR imaging. Magn Reson Med 1994; 32:43-51.

Santyr GE, Henkelman M, Bronskill MJ. Spin locking for magnetic resonance imaging with application to human breast. Magn Reson Med 1989; 12:25-37.

Schultz JF, Bell JD, Goldstein RM, Kuhn JA, McCarty TM. Hepatic tumor imaging using iron oxide MRI: comparison with computed tomography, clinical impact, and cost analysis. Ann Surg Oncol 1999; 6:691-698.

Semelka RC, Cance WG, Marcos HB, Mauro MA. Liver metastases: comparison of current MR techniques and spiral CT during arterial portography for detection in 20 surgically staged cases. Radiology 1999; 213:86-91.

Semelka RC, Worawattanakul S, Kelekis NL, John G, Woosley JT, Graham M, Cance WG. Liver lesion detection, characterization, and effect on patient management: comparison of single-phase spiral CT and current MR techniques. J Magn Reson Imaging 1997; 7:1040-1047.

Sepponen R. Rotating frame and magnetization transfer. In: Stark DD, Bradley WG.Jr (eds). Magnetic Resonance Imaging. Mosby Year Book, St. Louis, 1992, pp:204-218.

Sepponen RE, Korhola OA, Lamminen AE, Tanttu JI. Multiple-section spin-lock imaging: new high-contrast MR imaging technique. Radiology 1993; 189(P):320.

Sepponen RE, Sipponen JT, Tanttu JI. A method for chemical shift imaging: demonstration of bone marrow involvement with proton chemical shift imaging. J Comput Assist Tomogr 1984; 8:585-587.

Sepponen RE, Tanttu JI, Suramo I. T1ρ and T1ρ dispersion imaging in patients with cerebral infarction. Society of Magnetic Resonance in Medicine: Book of Abstracts, vol. 3, Fifth Annual Meeting, August 19-22, 1986, Montreal, Canada, p:639.

Shuman WP, Lambert DT, Patten RM, Baron RL, Tazioli PK. Improved fat suppression in STIR MR imaging: selecting inversion time through spectral display. Radiology 1991; 178:885-887.

Smith FW, Mallard JR, Hutchison JMS, Reid A, Johnson G, Redpath TW, Selbie RD. Clinical application of nuclear magnetic resonance. Lancet 1981a; 1:78-79.

Smith FW, Mallard JR, Reid A, Hutchison JMS. Nuclear magnetic resonance tomographic imaging in liver disease. Lancet 1981b; 1:963-966.

Stark DD, Weissleder R, Elizondo G, Hahn PF, Saini S, Todd LE, Wittenberg J, Ferrucci JT. Superparamagnetic iron oxide: clinical application as a contrast agent for MR imaging of the liver. Radiology 1988; 168:297-301.

Stark DD. Particulate iron oxide contrast agents for MR. In: Proceedings Contrast Media in MRI, international workshop, Berlin, February 1-3, 1990, pp:281-293.

Stark DD, Wittenberg J, Edelman RR, Middletonms, Saini S, Butch RJ, Brady TJ, Ferrucci, Jr JT. Detection of hepatic metastases: analysis of pulse sequence performance in MR imaging. Radiology 1986; 159:365-370.

Tang Y, Yamashita Y, Namimoto T, Takahashi M. Characterization of focal liver lesions with half-fourier acquisition single-shot turbo-spin-echo (HASTE) and inversion recovery (IR)-HASTE sequences. J Magn Reson Imaging 1998; 8:438-445.

Thomsen C, Christoffersen P, Henriksen O, Juhl E. Prolonged T1 in patients with liver cirrhosis: an in vivo MRI study. Magn Reson Imaging 1990; 8:599-604.

Tsang Y-M, Stark DD, Chia-Mei Chen M, Weissleder R, Wittenberg J, Ferrucci JT. Hepatic micrometastases in the rat: ferrite-enhanced MR imaging. Radiology 1988; 167:21-24.

Wang C. Mangafodipir trisodium (MnDPDP)-enhanced magnetic resonance imaging of the liver and pancreas. Acta Radiol 1998; 39 (S415):16.

Ward J, Chen F, Guthrie JA, Wilson D, Lodge JPA, Wyatt JI, Robinson PJ. Hepatic lesion detection after superparamagnetic iron oxide enhancement: comparison of five T2-weighted sequences at 1.0T by using alternative-free response receiver operating characteristic analysis. Radiology 2000; 214:159-166.

Ward J, Guthrie JA, Scott DJ, Atchley J, Wilson D, Davies MH, Wyatt JI, Robinson PJ. Hepatocellular carcinoma in the cirrhotic liver: double-contrast MR imaging for diagnosis. Radiology 2000; 216:154-162.

Wehrli FW. Fast-scan imaging: principles and contrast phenomenology. In: Higgins CB, Hricak H (eds.): Magnetic resonance imaging of the body. Raven Press, New York, 1987, pp:23-38.

Wehrli FW, MacFall JR, Glover GH, Grigsby N, Haughton V, Johanson J. The dependence of nuclear magnetic resonance (NMR) image contrast on intrinsic and pulse sequence timing parameters. Magn Reson Imaging 1984; 2:3-16.

Weissleder R, Stark DD, Engelstad BL, Bacon BR, Compton CC, White DL, Jacobs P, Lewis J. Superparamagnetic iron oxide: pharmacokinetics and toxicity. Am J Roentgenol 1989; 152:167-173.

Vilgrain V, van Beers BE, Flejou JF, Belghiti J, Delos M, Gautier AL, Zins M, Denys A, Menu Y. Intrahepatic cholangiocarcinoma: MRI and pathologic correlation of 14 patients. J Comput Assist Tomogr 1997; 21:59-65.

Villafana T. Fundamental physics of magnetic resonance imaging. Radiol Clin N Am 1988; 26:701-715.

Winter TC 3rd, Freeny PC, Nghiem HV, Mack LA, Patten RM, Thomas CR Jr, Elliott S. MR imaging with i.v. superparamagnetic iron oxide: efficacy in the detection of focal hepatic lesions. Am J Roentgenol 1993; 161:1191-1198.

Wittenberg J, Stark DD, Forman BH, Hahn PF, Saini S, Weissleder R, Rummeny E, Ferrucci JT. Differentiation of hepatic metastases from hepatic hemangiomas and cysts by using MR imaging. Am J Roentgenol 1988; 151:79-84.

Vogl TJ, Hamm B, Schnell B, McMahon C, Branding G, Lissner J, Wolf K-J. Mn-DPDP enhancement patterns of hepatocellular lesions on MR images. J Magn Reson Imaging 1993; 3:51-58.

Wolff SD and Balaban RS. Magnetization transfer contrast (MTC) and tissue water proton relaxation in vivo. Magn Reson Med 1989; 10:135-144.

Wolff SD, Chesnick S, Frank JA, Lim KO, Balaban RS. Magnetization transfer contrast: MR imaging of the knee. Radiology 1991; 179:623-628.

Worawattanakul S, Semelka RC, Noone TC, Calvo BE, Kelekis NL, Woosley JT. Cholangiocarcinoma: spectrum of appearances on MR images using current techniques. Magn Reson Imaging 1998; 16:993-1003.

Yamashita Y, Hatanaka Y, Yamamoto H, Arakawa A, Matsukawa T, Miyazaki T, Takahashi M. Differential diagnosis of focal liver lesions: role of spin-echo and contrast-enhanced dynamic MR imaging. Radiology 1994; 193:59-65.

Young IR, Bydder GM, Hajnal JV. Contrast properties of the inversion recovery sequence. In: Bradley WG, Bydder GM. (eds). Advanced MR imaging techniques, Mosby Year Book, St. Louis, 1998, pp:143-162.

Young SW, Bradley B, Muller HH, Rubin DL. Detection of hepatic malignancies using MnDPDP (manganese dipyridoxal diphosphate) hepatobiliary MRI contrast agent. Magn Reson Imaging 1990; 8:267-276.

Zhong JH, Gore JC, Armitage IM. Relative contributions of chemical exchange and other relaxation mechanisms in protein solutions and tissues. Magn Reson Med 1989; 11:295-308.

Zhong JH, Gore JC, Armitage IM. Quantitative studies of hydrodynamic effects and cross relaxation in protein solutions and tissues with proton and deuteron longitudinal relaxation times. Magn Reson Med 1990; 13:192-203.

APPENDIX

The equations used in the investigations included in the thesis are described below.

Studies I and II. The signal intensity (S) provided by the multiple slice SL sequence when gradient echo technique is used and the number of slices is large, and the flip angle small or intermediate may be calculated as follows:

$$S = \frac{\sin\alpha M_0 e^{-\frac{TE}{T2}}(1-e^{-\frac{TD}{T1}})e^{-\frac{TL}{T1\rho}}}{1-e^{-\frac{TD}{T1}}e^{-\frac{TL}{T1\rho}}},$$

where M_0 is the net magnetization, TD is the period between successive locking pulses, and TL is the length of the locking pulse.

The SL-effect (E_{SL}) was calculated as follows:

$$E_{SL} = SI_{SL\text{-}GE}/SI_{GE},$$

where the $SI_{SL\text{-}GE}$ and SI_{GE} are the signal intensities obtained from the multiple slice SL and GE images, respectively.

The MT-effect (E_{MT}) was determined by using follwing equation:

$$E_{MT} = SI_{MT\text{-}GE}/SI_{GE},$$

where $SI_{SL\text{-}GE}$, SI_{GE}, and $SI_{MT\text{-}GE}$ are the signal intensity values obtained from the respective MR images.

The diagnostic accuracies for the multiple slice SL and single slice MT techniques were detemined as follows:

The lesions *falsely* above or below the cut-off value were divided by all lesions included.

Study III. The SNR values for the liver parenchyma and the hepatic lesions were calculated followingly:

$$SNR=SI_{liver}/SD_{noise} \quad \text{and} \quad SNR=SI_{lesion}/SD_{noise},$$

where SI_{liver} and SI_{lesion} are the signal intensity values from the liver and the lesions, respectively and SD_{noise} is the standard deviation of the background noise. The CNR ratios were obtained by using the following equation:

$$CNR=(SI_{lesion}-SI_{liver})/ SD_{noise}.$$

Enhancement was defined with the equation:

$$(SNR_{pre}- SNR_{post})/SNR_{pre},$$

where SNR_{pre} and SNR_{post} are the signal-to-noise ratios in the precontrast and postcontrast images, respectively.

Study IV. Hepatic enhancement (E%) was defined as follows:

$$E(\%)=[(SNR_{post}-SNR_{pre})/SNR_{pre}]x100,$$

where SNR_{pre} and SNR_{post} are the signal-to-noise ratios in the corresponding pre- and postcontrast images.

The CNR values were calculated similarly as in the **Study III**.